A Review of Target Decomposition Theorems in Radar Polarimetry

Shane Robert Cloude, *Member, IEEE,* and Eric Pottier, *Member, IEEE*

Abstract— **In this paper, we provide a review of the different approaches used for target decomposition theory in radar polarimetry. We classify three main types of theorem: those based on the Mueller matrix and Stokes vector, those using an eigenvector analysis of the covariance or coherency matrix, and those employing coherent decomposition of the scattering matrix. We unify the formulation of these different approaches using transformation theory and an eigenvector analysis. We show how special forms of these decompositions apply for the important case of backscatter from terrain with generic symmetries.**

I. Introduction

THERE is currently a great deal of interest in the use of polarimetry for radar remote sensing. In this context, an important objective is to extract physical information from the observed scattering of microwaves by surface and volume structures. The most important observable measured by such radar systems is the 3×3 coherency matrix or equivalent 4×4 Mueller matrix. This paper addresses a set of methods known collectively as target decomposition theorems which have been developed for the interpretation of such data. Note that we distinguish the problems of interpretation and estimation of the Mueller matrix. The multiplicative noise known as speckle makes the latter a nontrivial exercise (see [1] for details on how to provide optimum estimates of matrices in the presence of speckle). In this paper we restrict attention to the former problem of interpretation of information in the estimated scattering matrix.

Target decomposition (TD) theorems were first formalized by Huynen [2] but have their roots in the work of Chandrasekhar on light scattering [3] by small anisotropic particles. Since this original work, there have been many other proposed decompositions. In this paper we provide a review of the different approaches and highlight details of their algorithmic implementation. We conclude with a suggested unified framework for the application of TD theorems to radar data.

Many targets of interest in radar remote sensing require a multivariate statistical description due to the combination of coherent speckle noise and random vector scattering effects from surface and volume. For such targets, it is of interest to generate the concept of an average or dominant scattering mechanism for the purposes of classification or inversion of scattering data. TD theorems are aimed at providing such an interpretation based on sensible physical constraints such as the average target being invariant to changes in wave polarization base.

The theory of vector radiative transfer (VRT) is widely used to model wave propagation in anisotropic random particle clouds. The elements of this theory were first outlined in the book by Chandrasekhar [3] (a more modern treatment is available in the book by Tsang [4]). According to this theory, a polarized wave interacts with a cloud of discrete scatterers through a combination of wave propagation, attenuation, and scattering. The balance of these processes is formally presented by an integro-differential equation for the four element specific intensity vector g (which is related to the classical Stokes vector of the wave) as shown in (1)

$$\frac{d\underline{g}(\underline{r}, \underline{s})}{ds} = -[\kappa_e].\underline{g}(\underline{r}, \underline{s}) + \int_{4\pi} [R(\underline{r}, \underline{s}, \underline{s}')].\underline{g}(\underline{r}, \underline{s}')\, d\Omega' \quad (1)$$

where $[\kappa_e]$ is a 4×4 extinction matrix and $[R]$ is the phase matrix, which dictates the scattering of specific intensity from direction $\underline{s}'$ into direction $\underline{s}$.

The solution of (1) leads to a Mueller matrix relationship between the Stokes vectors for the incident and scattered wave directions (Fig. 1 and (2))

$$\underline{g}_s = [M]\underline{g}_i. \quad (2)$$

The 4×4 real matrix $[M]$ forms the central concern of this paper.

One of the simplest scattering problems to consider is that from a cloud of Rayleigh scatterers, i.e., scattering by electrically small isotropic particles. For this case, Chandrasekhar [3] gives the phase matrix in the form shown in (3)

$$[R] = \frac{3}{2}\begin{bmatrix} \cos^2\theta & 0 & 0 & 0 \\ 0 & 1 & 0 & 0 \\ 0 & 0 & \cos\theta & 0 \\ 0 & 0 & 0 & \cos\theta \end{bmatrix}$$
$$\underline{g} = [I_{||} \quad I_{\perp} \quad U \quad V]^T \quad (3)$$

where θ is the scattering angle in the scattering plane as shown in Fig. 1 ($\theta = 0°$ is forward scatter and $\theta = 180°$ is backscatter). Note that the Stokes vector $\underline{g}$ is expressed in terms of the modified Stokes parameters. More commonly in radar, use is made of the Stokes vector $(I, Q, U, V)^T$, where the two different wave vectors are related by (4)

$$\begin{bmatrix} I_{||} \\ I_{\perp} \\ U \\ V \end{bmatrix} = \begin{bmatrix} 1 & 1 & 0 & 0 \\ 1 & -1 & 0 & 0 \\ 0 & 0 & 1 & 0 \\ 0 & 0 & 0 & 1 \end{bmatrix} \begin{bmatrix} I \\ Q \\ U \\ V \end{bmatrix}. \quad (4)$$

Manuscript received February 16, 1995; revised August 29, 1995.

The authors are with the SEI EP CNRS 63 Laboratory, IRESTE, La Chantrerie, 44087 Nantes, France (e-mail: epottier@ireste.fr).

Publisher Item Identifier S 0196-2892(96)01003-0.

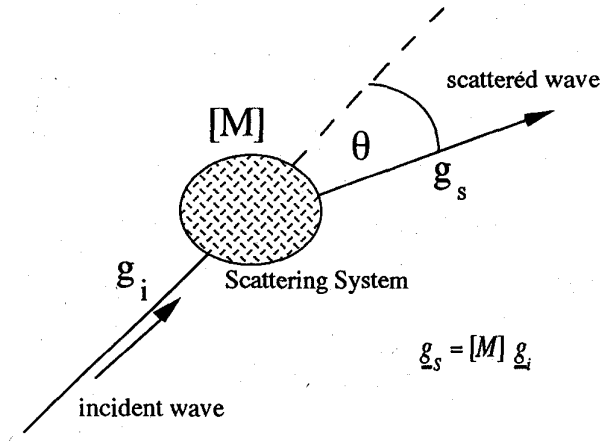

Fig. 1. General scattering geometry for Stokes vectors.

Chandrasekhar went on to consider the more difficult problem of scattering by a cloud of small anisotropic particles (such as ellipsoids) and showed that the phase matrix could be represented as shown in (5)

$$[R] = \frac{3}{2(1+2\gamma)} \cdot \begin{bmatrix} \cos^2\theta + \gamma\sin^2\theta & \gamma & 0 & 0 \\ \gamma & 1 & 0 & 0 \\ 0 & 0 & (1-\gamma)\cos\theta & 0 \\ 0 & 0 & 0 & (1-3\gamma)\cos\theta \end{bmatrix} \tag{5}$$

where γ is a single parameter which accounts for the anisotropy of the particles ($\gamma = 0$ reduces to the case for Rayleigh scattering). Chandrasekhar then points out that we can consider this matrix as the sum of three independent elements (6)

$$[R] = \frac{3(1-\gamma)}{2(1+2\gamma)} \begin{bmatrix} \cos^2\theta & 0 & 0 & 0 \\ 0 & 1 & 0 & 0 \\ 0 & 0 & \cos\theta & 0 \\ 0 & 0 & 0 & 0 \end{bmatrix} + \frac{3\gamma}{2(1+2\gamma)} \begin{bmatrix} 1 & 1 & 0 & 0 \\ 1 & 1 & 0 & 0 \\ 0 & 0 & 0 & 0 \\ 0 & 0 & 0 & 0 \end{bmatrix} + \frac{3(1-3\gamma)}{2(1+2\gamma)} \begin{bmatrix} 0 & 0 & 0 & 0 \\ 0 & 0 & 0 & 0 \\ 0 & 0 & 0 & 0 \\ 0 & 0 & 0 & \cos\theta \end{bmatrix}. \tag{6}$$

The third component is a scalar transformation of the V parameter. However, the first and second yield an interesting physical interpretation of the polarimetric part of the problem. We see that the first matrix is proportional to the top 3×3 portion of (3), i.e., it represents a Rayleigh scattering term. The second element is a randomly polarized "noise" term (by noise we mean that the power generated by this element is independent of the choice of wave polarization state). Note that this noise term disappears for the case of isotropic scatterers ($\gamma = 0$).

In this case, we can decompose the problem of scattering by small anisotropic particles into conventional Rayleigh scatter with the addition of a noise term (due to the particle anisotropy). This example illustrates the main idea behind TD theorems: to express the average scattering matrix for a random media problem as a sum of independent elements and to associate a physical mechanism with each component.

The above example is the first documented example of such a decomposition (although related work has been carried out in the former Soviet Union (see [5]), the authors are not aware of any developments related to Target Decomposition which predate this example). The question as to whether such an approach could be generalized to other scattering problems was first addressed by Huynen in his Ph.D. dissertation [2]. Before considering the details of his approach, we first establish some notation and define two important concepts; that of polarimetric fluctuation statistics and conditions for a random target to have a single coherent scattering matrix representation.

II. Polarization Scattering Matrices

A. Target Vectors for Backscatter Problems

An important recent development in our understanding of how to best extract physical information from the classical 2×2 coherent scattering matrix $[S]$ (see [6] and [7] for basic definitions) has been through the construction of system vectors [8], [9]. We represent this vectorization of a matrix by the operator $V(..)$ such that

$$\begin{aligned} [S] = \begin{bmatrix} S_{xx} & S_{xy} \\ S_{yx} & S_{yy} \end{bmatrix} \Rightarrow \\ \underline{k} &= V([S]) \\ &= \tfrac{1}{2}\,\mathrm{Trace}\,([S]\Psi) \\ &= (k_0 \quad k_1 \quad k_2 \quad k_3)^T \quad \underline{k} \in C_4 \end{aligned} \tag{7}$$

where $\mathrm{Trace}\,([A])$ is the sum of diagonal elements of matrix $[A]$ and Ψ are a set of 2×2 complex basis matrices which are constructed as an orthonormal set under an hermitian inner product. Several different basis sets have been used in the literature; two important examples are shown in (8)

$$\begin{aligned} &\psi_L \begin{bmatrix} 2 & 0 \\ 0 & 0 \end{bmatrix} \begin{bmatrix} 0 & 2 \\ 0 & 0 \end{bmatrix} \begin{bmatrix} 0 & 0 \\ 2 & 0 \end{bmatrix} \begin{bmatrix} 0 & 0 \\ 0 & 2 \end{bmatrix}; \\ &\psi_P \sqrt{2} \begin{bmatrix} 1 & 0 \\ 0 & 1 \end{bmatrix} \sqrt{2} \begin{bmatrix} 1 & 0 \\ 0 & -1 \end{bmatrix} \sqrt{2} \begin{bmatrix} 0 & 1 \\ 1 & 0 \end{bmatrix} \sqrt{2} \begin{bmatrix} 0 & -i \\ i & 0 \end{bmatrix} \end{aligned} \tag{8}$$

where ψ_L is a straightforward lexicographic ordering of the elements of $[S]$ and ψ_P is based on special linear combinations arising from the Pauli matrices (the factor of $\sqrt{2}$ arises from the requirement to keep $\mathrm{Trace}([S][S]^\dagger)$ an invariant; namely the total power scattered by the target). The target vectors in these bases have the explicit form shown in (9)

$$\begin{aligned} &\underline{k}_P = \\ &\frac{1}{\sqrt{2}}[S_{xx} + S_{yy} \quad S_{xx} - S_{yy} \quad S_{xy} + S_{yx} \quad i(S_{xy} - S_{yx})]^T \\ &\underline{k}_L = [S_{xx} \quad S_{xy} \quad S_{yx} \quad S_{yy}]^T. \end{aligned} \tag{9}$$

With such a vectorization we can then generate a coherency matrix from the outer product of a $\underline{k}$ vector with its conjugate transpose (or adjoint vector) so that in the ψ_P representation we can define

$$[T] = \underline{k}_P . \underline{k}_P^{*T} = \begin{bmatrix} A_0 + A & C - iD & H + iG & I - iJ \\ C + iD & B_0 + B & E + iF & K - iL \\ H - iG & E - iF & B_0 - B & M + iN \\ I + iJ & K + iL & M - iN & A_0 - A \end{bmatrix} = [T]^{\dagger} \tag{10}$$

where the reason for the parameterization in terms of the letters A, B, C, $\cdots$, etc., will become more apparent when we calculate the form of the Mueller matrix $[M]$ corresponding to $[T]$ (12). The relationship between $[M]$ and $[T]$ has been developed by many authors (see [8]) and can be succinctly represented in the form shown in (11)

$$\begin{aligned} m_{ij} &= \tfrac{1}{2} \operatorname{Trace}([T]\eta_{4i+j}) \\ \eta_{4i+j} &= (-1)^{-\delta_{3j}} [A]\sigma_i \otimes \sigma_j [A]^{*T} \\ [A] &= \frac{1}{\sqrt{2}} \begin{bmatrix} 1 & 0 & 0 & 1 \\ 1 & 0 & 0 & -1 \\ 0 & 1 & 1 & 0 \\ 0 & i & -i & 0 \end{bmatrix} \\ \delta_{ij} &= \begin{cases} 0 & i \neq j \\ 1 & i = j. \end{cases} \end{aligned} \tag{11}$$

$$\sigma_0 = \begin{bmatrix} 1 & 0 \\ 0 & 1 \end{bmatrix}, \ \sigma_1 = \begin{bmatrix} 1 & 0 \\ 0 & -1 \end{bmatrix}$$
$$\sigma_2 = \begin{bmatrix} 0 & 1 \\ 1 & 0 \end{bmatrix}, \ \sigma_3 = \begin{bmatrix} 0 & -i \\ i & 0 \end{bmatrix}.$$

The four matrices σ_i $(i = 0, 1, 2, 3)$ are called the Pauli spin matrices following their original application in a description of spin in quantum mechanics. As we shall see in this paper, they are also of great importance in a description of polarized wave interactions.

When we insert (10) into (11), the Mueller matrix has the form

$$[M] = \begin{bmatrix} A_0 + B_0 & C + N & H + L & F + I \\ C - N & A + B & E + J & G + K \\ H - L & E - J & A - B & D + M \\ I - F & K - G & M - D & A_0 - B_0 \end{bmatrix}. \tag{12}$$

In this case, we can see for example that C and D, although separated in the Mueller matrix, relate to the real and imaginary parts of a complex product of $[S]$ matrix terms, namely $(S_{xx} + S_{yy})(S_{xx} - S_{yy})^*$. It turns out that from electromagnetic scattering theory, such linear combinations and their correlations are more closely related to physical properties of the scattering medium [16].

If we alternatively use the base ψ_L to generate a vector $\underline{k}_L$ and represent the corresponding 4×4 hermitian matrix as $[C]$, then we can easily show that the matrices $[C]$ and $[T]$ are related by the transformation

$$[C] = [A]^{*T}[T][A] = \tfrac{1}{2} \begin{bmatrix} 1 & 1 & 0 & 0 \\ 0 & 0 & 1 & -i \\ 0 & 0 & 1 & i \\ 1 & -1 & 0 & 0 \end{bmatrix} [T] \begin{bmatrix} 1 & 0 & 0 & 1 \\ 1 & 0 & 0 & -1 \\ 0 & 1 & 1 & 0 \\ 0 & i & -i & 0 \end{bmatrix}. \tag{13}$$

The matrix $[C]$ is called the target covariance matrix and is to be distinguished from the coherency matrix $[T]$. However, these two matrices share some interesting properties. For example, both are hermitian positive semidefinite and have the same eigenvalues (since the transformation in (13) is a unitary similarity transformation). The eigenvectors of both $[C]$ and $[T]$ form orthonormal sets of vectors which can be used as a suitable basis for the vectorization $V([S])$ of (7).

In many applications, such as radar remote sensing, interest centers on the backscatter direction for which the dimensionality of the above polarization matrices reduces. In radar remote sensing, we also encounter some special problems associated with wave coordinates. For backscatter, the vector reciprocity theorem forces the scattering matrix to be antisymmetric [34] (for a right handed coordinate system which follows the wave propagation), i.e.,

$$[S] = \begin{bmatrix} a & b \\ -b & d \end{bmatrix} \Rightarrow \underline{k}_P = \frac{1}{\sqrt{2}} (a + d \quad a - d \quad 0 \quad 2ib)^T \tag{14}$$

in which special case the coherency matrix has the general form

$$[T] = \begin{bmatrix} A_0 + A & C - iD & 0 & I - iJ \\ C + iD & B_0 + B_0 & 0 & K - iL \\ 0 & 0 & 0 & 0 \\ I + iJ & K + iL & 0 & A_0 - A \end{bmatrix} \Rightarrow [T_3] = \begin{bmatrix} A_0 + A & C - iD & I - iJ \\ C + iD & 2B_0 & K - iL \\ I + iJ & K + iL & A_0 - A \end{bmatrix} \tag{15}$$

and the Mueller matrix for backscatter has the form

$$[M] = \begin{bmatrix} A_0 + B_0 & C & L & I \\ C & A + B_0 & J & K \\ -L & -J & A - B_0 & D \\ I & K & -D & A_0 - B_0 \end{bmatrix}. \tag{16}$$

In the radar community, a coordinate change is often used so that by international agreement a right handed coordinate system is used for transmitted waves and a left handed for receive [21] (this rather awkward notation simplifies the definition of antenna properties in communications and radar). Fig. 2 shows a simplified representation of the two coordinate systems.

The antenna coordinate system has the effect of changing the detailed form of the polarization matrices and in particular it makes the backscatter matrix $[S_A]$ symmetric. It has the advantage that rotations through angle θ are the same in both transmit and receive coordinate systems, whereas for the wave coordinates we must change the sign of θ in matrix transformations (see Fig. 2).

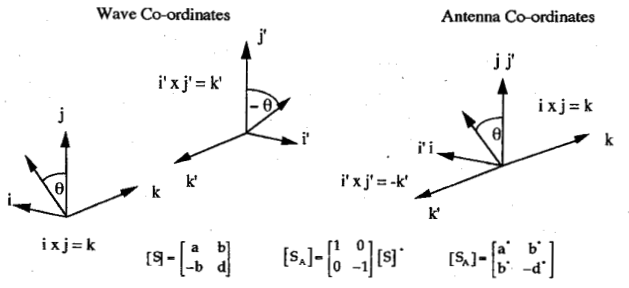

Fig. 2. Coordinate systems used in backscatter problems.

In the antenna coordinate system we then have the following special form for the target vector, coherency and Mueller matrices (we use a subscript A to denote the use of antenna coordinates)

$$[S_A] = \begin{bmatrix} a & b \\ b & e \end{bmatrix} \Rightarrow$$

$$\underline{k}_A = \frac{1}{\sqrt{2}} [a+e \quad a-e \quad 2b \quad 0]^T \tag{17}$$

$$[T_A] = \begin{bmatrix} 2A_0 & C-iD & H+iG & 0 \\ C+iD & B_0+B & E+iF & 0 \\ H-iG & E-iF & B_0-B & 0 \\ 0 & 0 & 0 & 0 \end{bmatrix} \Rightarrow$$

$$[T_{3A}] = \begin{bmatrix} 2A_0 & C-iD & H+iG \\ C+iD & B_0+B & E+iF \\ H-iG & E-iF & B_0-B \end{bmatrix} \tag{18}$$

$$[M_A] = \begin{bmatrix} A_0+B_0 & C & H & F \\ C & A_0+B & E & G \\ H & E & A_0-B & D \\ F & G & D & -A_0+B_0 \end{bmatrix} \tag{19}$$

where the last row of $[M_A]$ has been multiplied by -1 in order to account for the conjugate operation shown in $[S_A]$ in Fig. 2 (this conjugate operation is due to the fact that the propagation vectors k and k' point in opposite directions, and hence, the sense of circular polarization is reversed). Note that in this special coordinate system, the Mueller matrix is real symmetric. To distinguish these coordinate transformations, in the radar literature the matrix $[M_A]$ is often called the Kennaugh matrix [21], named after one of the first scientists to consider the application of polarization techniques to radar.

For backscatter, a reduced target vector in the ψ_L base is often used and has the form

$$k_{3L} = [S_{xx} \quad \sqrt{2}S_{xy} \quad S_{yy}]^T. \tag{20}$$

Note the factor of $\sqrt{2}$, which is required in order to keep the vector norm consistent with the span invariance of (8). The 3×3 coherency matrix $[T_{3A}]$ is then related to a 3×3 covariance matrix $[C_{3A}]$ as

$$[C_{3A}] = \frac{1}{2} \begin{bmatrix} 1 & 1 & 0 \\ 0 & 0 & \sqrt{2} \\ 1 & -1 & 0 \end{bmatrix} [T_{3A}] \begin{bmatrix} 1 & 0 & 1 \\ 1 & 0 & -1 \\ 0 & \sqrt{2} & 0 \end{bmatrix}. \tag{21}$$

These matrices form the starting point for our analysis of TD theorems.

B. Conditions for Single Matrix Representations

Equation (19) introduced a parameterization of the target Mueller matrix in the antenna coordinates. Such a matrix governs the change of Stokes vector from the incident to scattered waves (2) so that

$$\underline{g}_s = \begin{bmatrix} I_s \\ Q_s \\ U_s \\ V_s \end{bmatrix} = \begin{bmatrix} A_0+B_0 & C & H & F \\ C & A_0+B & E & G \\ H & E & A_0-B & D \\ F & G & D & B_0-A_0 \end{bmatrix} \begin{bmatrix} I_i \\ Q_i \\ U_i \\ V_i \end{bmatrix} = \langle [M_A] \rangle \underline{g}_i. \tag{22}$$

It is well known that the Stokes vector can be used to represent partially polarized waves with a degree of polarization less than one [10]. It follows that not every matrix $\langle [M_A] \rangle$ has a single corresponding $[S_A]$ matrix (since by definition $[S_A]$ matrices generate only purely polarized waves with unit degree of polarization). It is a central objective of TD theorems to identify the circumstances under which a measured Mueller matrix has a single corresponding $[S_A]$ matrix.

We can see from (17)–(19) that the condition for $\langle [M_A] \rangle$ to have such an equivalent $[S_A]$ is for the coherency matrix $\langle [T_A] \rangle$ to have rank $r = 1$. In this case, the matrix $\langle [T_A] \rangle$ can be expressed as the outer product of a *single* target vector $\underline{k}_A$, in which case $\langle [M_A] \rangle$ has a single equivalent $[S_A]$, i.e.,

$$\langle [T_A] \rangle = \underline{k}_A \underline{k}_A^{*T} \Rightarrow \langle [M_A] \rangle \equiv [S_A]. \tag{23}$$

This criterion is very much simpler to use than those based on conditions on the elements of $\langle [M_A] \rangle$ itself [2], [11]–[13]. These alternative forms of the conditions can be derived from $\langle [T_{3A}] \rangle$ in (18) by noting that for rank 1 matrices, all principal minors of the matrix must equal zero. By calculating these minors we then obtain a set of constraints on the elements $A, B, C, \cdots$, etc.

For example, when we restrict consideration to backscatter and the matrix $[M_A]$, Huynen [2] was the first to show that for the $[M_A]$ matrix to have a corresponding single $[S_A]$ matrix requires that the three equalities in (24) hold:

$$\begin{aligned} 2A_0(B_0+B) &= C^2+D^2 \\ 2A_0(B_0-B) &= H^2+G^2 \\ B_0^2-B^2 &= E^2+F^2. \end{aligned} \tag{24}$$

These are obtained directly from the 2×2 principal minors of $[T_A]$ in (18). Similar but more complicated relations exist for the general Mueller matrix [11], [12]. In practice, it is easier to consider these conditions by examining the rank of $\langle [T] \rangle$ rather than by using (24) or their generalization to arbitrary scattering angles. It follows that if in general $\langle [T] \rangle$ has only one nonzero eigenvalue, then $\langle [M] \rangle$ has a single equivalent $[S]$ matrix. Further, if $\langle [T] \rangle$ is positive semidefinite (PSD) then $\langle [M] \rangle$ represents a general Mueller matrix which satisfies the Stokes criterion [11]–[13].

Such considerations are of secondary importance for radar systems where the coherent matrix $[S]$ is measured directly,

since by construction $\langle[T]\rangle$ will always be PSD. However, for radars employing a Stokes vector receiver such considerations are very important for establishing the quality of the data, since in these cases there is no guarantee that $\langle[T]\rangle$ will be PSD (due to system noise, e.g., [50], [51]).

C. Statistical Fluctuations of Target Vectors

In random media problems, such as those treated by VRT, interest centers not so much on the target vectors $\underline{k}$ but on averages over fluctuations of the elements of $\underline{k}$. If important correlations survive such averaging then we can use these to identify and classify structure in the scattering problem from measurement of the coherency matrix of fluctuations as shown below.

We consider fluctuations in the elements of $\underline{k} = \underline{k}_P$ (9) such that

$$\begin{aligned} \underline{k} &= \underline{k}_m + \Delta\underline{k} \\ E(\Delta\underline{k}) &= 0. \end{aligned} \tag{25}$$

The coherency matrix of such a vector can be obtained from (10) as

$$\begin{aligned} [T] &= \underline{k}^\dagger \underline{k} \\ &= (\underline{k}_m + \Delta\underline{k}).(\underline{k}_m^\dagger + \Delta\underline{k}^\dagger) \\ &= [T_m] + \underline{k}_m \Delta\underline{k}^\dagger + \Delta\underline{k}^\dagger \underline{k}_m + \Delta\underline{k}\Delta\underline{k}^\dagger. \end{aligned} \tag{26}$$

Note that this matrix is rank 1, i.e., it is a single target matrix and has a Mueller matrix with a corresponding phase unique scattering matrix $[S]$. Now let us average over an ensemble of such vectors. We then obtain the averaged matrix $\langle[T]\rangle$ as

$$\begin{aligned} \langle[T]\rangle &= \langle[T_m]\rangle + \langle \underline{k}_m \Delta\underline{k}^\dagger + \Delta\underline{k}^\dagger \underline{k}_m \rangle + \langle \Delta\underline{k}\Delta\underline{k}^\dagger \rangle \\ &= [T_m] + \langle \Delta\underline{k}\Delta\underline{k}^\dagger \rangle \end{aligned} \tag{27}$$

where $\langle[T]\rangle$ has rank $r \geq 1$ but $[T_m]$ has rank $r = 1$. From this we can define a coherency matrix of fluctuations as

$$\langle \Delta\underline{k}\Delta\underline{k}^\dagger \rangle = \langle[T_f]\rangle. \tag{28}$$

We shall show that for the Huynen Decomposition (see (39)) this matrix has the special form

$$\langle[T_f]\rangle = \begin{bmatrix} 0 & 0 & 0 \\ 0 & \alpha & \beta \\ 0 & \beta^* & \gamma \end{bmatrix} \tag{29}$$

so that from (21) we have

$$\begin{aligned} \langle[C]\rangle &= \tfrac{1}{2} \begin{bmatrix} 1 & 1 & 0 \\ 0 & 0 & \sqrt{2} \\ 1 & -1 & 0 \end{bmatrix} \begin{bmatrix} 0 & 0 & 0 \\ 0 & \alpha & \beta \\ 0 & \beta^* & \gamma \end{bmatrix} \begin{bmatrix} 1 & 0 & 1 \\ 1 & 0 & -1 \\ 0 & \sqrt{2} & 0 \end{bmatrix} \\ &= \tfrac{1}{2} \begin{bmatrix} \alpha & \sqrt{2}\beta & -\alpha \\ \sqrt{2}\beta^* & 2\gamma & -\sqrt{2}\beta^* \\ -\alpha & -\sqrt{2}\beta & \alpha \end{bmatrix}. \end{aligned} \tag{30}$$

From (30), we see that for a Huynen decomposition to apply requires a negative correlation between S_{hh} and S_{vv}. Such a fluctuation cannot be considered generic to the statistics of radar signals and so the Huynen decomposition (like the Chandrasekhar decomposition) must be considered a special case of a wider class of problems. Nonetheless, the concepts involved in establishing this decomposition will permit us to extend the approach to general scattering problems.

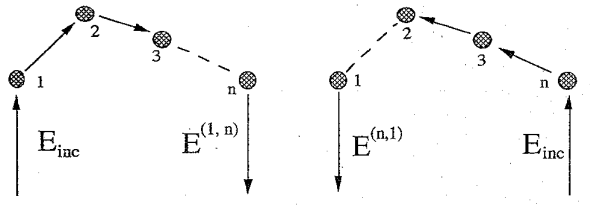

Fig. 3. Multiple scattering from a cloud of particles.

Before considering the Huynen decomposition in detail, we first examine another decomposition of the coherency matrix which has importance for the application of VRT to backscatter problems.

D. Mischenko Decomposition and VRT

As an example of the application of the target vector formalism to random media scattering, we now consider the problem of multiple scattering from a cloud of particles and show how the target coherency concept can be applied to classical vector radiative transfer theory. We consider the special but important case of multiple backscatter from low loss media as shown in Fig. 3.

Note that in this section, we abandon use of the antenna coordinates, since for multiple scattering it is better to use a wave coordinate system to multiply the scattering matrices for the various contributions. As shown by Mischenko [14], this problem has three important physical components. The first is single scattering from a random distribution of particles. The second is multiple incoherent scattering due to the ladder terms in an expansion of the multiple scattering integral equations [4]. This yields a diffuse or noncoherent background. This ladder component can be calculated using classical vector radiative transfer theory.

The third component arises from coherence (in the exact backscatter direction) between a path and its time reversed contribution as shown in Fig. 3 [14], [15]. In multiple scattering terms, this contribution arises from the sum of cyclical components in the integral equation. This term is difficult to calculate for a general random medium problem but Mischenko [14] has shown that for backscatter, there is a simple but important relationship between the coherent and noncoherent multiple scattering contributions.

In general terms, we can expand the Mueller matrix for this system as

$$\langle[M]\rangle = \langle[M_s]\rangle + \langle[M_L]\rangle + \langle[M_C]\rangle \tag{31}$$

where the subscripts s stands for single scattering, L for the ladder terms, and C for cyclical terms. This constitutes a class of decomposition theorem based on independent scattering processes. Further, since there is a one-to-one correspondence between each $\langle[M]\rangle$ and a coherency matrix $\langle[T]\rangle$ (see (10)

and (11)), we can rewrite this as

$$\begin{aligned}\langle[T]\rangle &= \langle[T_s]\rangle + \langle[T_L]\rangle + \langle[T_C]\rangle \\ &= \langle[T_s]\rangle + \langle[T_M]\rangle. \end{aligned} \tag{32}$$

Mischenko obtains his important relationship between $\langle[T_L]\rangle$ and $\langle[T_C]\rangle$ by using the vector reciprocity theorem. In terms of target vectors we can write the contribution to the backscattered field in the form

$$\begin{aligned}\langle[T_M]\rangle &= \langle[\underline{k}_{(1,n)} + \underline{k}_{(n,1)}][\underline{k}^{*T}_{(1,n)} + \underline{k}^{*T}_{(n,1)}]\rangle \\ &= \langle\underline{k}_{(1,n)}\underline{k}^{*T}_{(1,n)} + \underline{k}_{(n,1)}\underline{k}^{*T}_{(n,1)} \\ &\quad + \underline{k}_{(1,n)}\underline{k}^{*T}_{(n,1)} + \underline{k}_{(n,1)}\underline{k}^{*T}_{(1,n)}\rangle \\ &= \langle\underline{k}_{(1,n)}\underline{k}^{*T}_{(1,n)} + \underline{k}_{(n,1)}\underline{k}^{*T}_{(n,1)}\rangle \\ &\quad + \langle\underline{k}_{(1,n)}\underline{k}^{*T}_{(n,1)} + \underline{k}_{(n,1)}\underline{k}^{*T}_{(1,n)}\rangle \\ &= \langle T_L\rangle + \langle T_C\rangle. \end{aligned} \tag{33}$$

where we see that the cyclical terms arise from the cross coupling between system vectors for the two paths (these cross terms are by definition zero for the ladder contributions). The main result follows from the observation that the two system vectors $\underline{k}_{(1,n)}$ and $\underline{k}_{(n,1)}$ (Fig. 3) are of the form

$$\begin{aligned}\underline{k}_{(1,n)} &= (k_1 \quad k_2 \quad k_3 \quad k_4)^T \Rightarrow \\ \underline{k}_{(n,1)} &= (k_1 \quad k_2 \quad -k_3 \quad k_4)^T \end{aligned} \tag{34}$$

where the minus sign arises since the scattering matrices for paths $(1, n)$ and $(n, 1)$ are related by the vector reciprocity theorem as

$$[S_{(1,n)}] = \begin{bmatrix}1 & 0\\ 0 & -1\end{bmatrix}[S_{(n,1)}]^T\begin{bmatrix}1 & 0\\ 0 & -1\end{bmatrix} \tag{35}$$

where the coherent matrix $[S_{(n,1)}]$ is formed as a product of n particle scattering matrices for the multiple scattering path (and is not necessarily symmetric). Note that (34) simply arises from the constraint that for backscatter, the overall scattering matrix must be antisymmetric (14). In terms of coherency matrices it then easily follows from (33) and (34) that

$$\begin{aligned}\langle[T_L]\rangle &= \begin{bmatrix}t_{11} & t_{12} & 0 & t_{14}\\ t_{21} & t_{22} & 0 & t_{24}\\ 0 & 0 & t_{33} & 0\\ t_{41} & t_{42} & 0 & t_{44}\end{bmatrix} \Rightarrow \\ \langle[T_C]\rangle &= \begin{bmatrix}t_{11} & t_{12} & 0 & t_{14}\\ t_{21} & t_{22} & 0 & t_{24}\\ 0 & 0 & -t_{33} & 0\\ t_{41} & t_{42} & 0 & t_{44}\end{bmatrix}. \end{aligned} \tag{36}$$

This result ensures that the observed coherency matrix is 3×3, as expected for backscatter problems. However, from (36) it follows that if we can calculate the ladder terms for backscatter, then we can immediately obtain the contribution of the cyclic terms (simply by changing the sign of the 3, 3 element in $\langle[T]\rangle$). As noted earlier, the ladder terms can be calculated using conventional vector radiative transfer theory and so this result means that we can use the same theory to calculate the cyclical terms in the backscatter direction. For other scattering angles, the calculation of $\langle[T_C]\rangle$ poses severe difficulties because of the need to preserve coherence. Some implications of this result for remote sensing applications have recently been explored by Mishchenko and Hovenier [49].

Here we have seen yet another example where decomposition of the system Mueller matrix into component parts leads to increased computational efficiency and physical insight. We now turn to a more systematic treatment of such decompositions, beginning with the Huynen approach.

III. Huynen Type Decompositions

In his Ph.D. dissertation, Huynen [2] attempted the first systematic generalization of this concept of expressing the Mueller matrix as the sum of independent elements. The two key elements he used were as follows:

1) to consider distributed targets for which the Mueller matrix $\langle[M_A]\rangle$ has no single equivalent $[S_A]$ matrix and target vector fluctuations occur as described in (25);
2) to try and extract from this average a Mueller matrix component $[M_s]$, which has a corresponding rank one coherency matrix and so an equivalent single $[S_A]$ matrix. The remainder matrix is also to be a Mueller matrix but for a distributed, not a single target. This remainder he called an N-target (for nonsymmetric target). This remainder is not arbitrary, but is to satisfy invariance of form after rotation of the antenna coordinate system about the line of sight.

Huynen's original idea was based on the postulated existence of a target dichotomy to parallel the well known wave dichotomy [10], [16]; this lead him to his single target plus N-target residue theorem whereby we express an arbitrary Mueller matrix $[M_A]$ in the form shown in (37) and (38)

$$\langle[M_A]\rangle = [M_s] + \langle[M_N]\rangle \tag{37}$$

$$\begin{aligned}\langle[M_A]\rangle &= \begin{bmatrix}A_0 + B_0^S & C & H & F^S\\ C & A_0 + B^S & E^S & G\\ H & E^S & A_0 - B^S & D\\ F^S & G & D & B_0^S - A_0\end{bmatrix} \\ &\quad + \begin{bmatrix}B_0^N & 0 & 0 & F^N\\ 0 & B^N & E^N & 0\\ 0 & E^N & -B^N & 0\\ F^N & 0 & 0 & B_0^N\end{bmatrix}. \end{aligned} \tag{38}$$

The parameters A_0, C, H, G, and D are fixed and the others chosen so as to satisfy the constraint that $[M_s]$ have an equivalent rank one coherency matrix and so a single scattering matrix $[S_A]$. From Section II-B, we have seen that it is more convenient to enforce this using the coherency matrix formulation.

We can equally formulate the Huynen Decomposition in terms of the target coherency matrix $\langle[T]\rangle$, as shown in (39). The symbol x represents the appropriate element of $\langle[T]\rangle$ and α_1, α_3 are real, and α_2 complex. The coefficients are chosen to ensure that the matrix $[T_s]$ has rank 1:

$$\begin{aligned}\langle[T_{3A}]\rangle &= [T_s] + \langle[T_N]\rangle \\ &= \begin{bmatrix}x & x & x\\ x & x-\alpha_1 & x-\alpha_2\\ x & x-\alpha_2^* & x-\alpha_3\end{bmatrix} + \begin{bmatrix}0 & 0 & 0\\ 0 & \alpha_1 & \alpha_2\\ 0 & \alpha_2^* & \alpha_3\end{bmatrix}. \end{aligned} \tag{39}$$

This represents the most succinct form of the Huynen decomposition as a special factorization of the coherency matrix. This factorization was not made arbitrarily, but follows from

consideration of the properties of the coherency matrix under a restricted unitary transformation of the type shown in (40). This transformation represents a rotation of the target about the line of sight (in the antenna coordinate system) and Huynen's prime concern was to make the form of the N-target residue invariant under such roll transformations, i.e., $\langle[T_N]\rangle$ remains of the form shown on the far right hand side of (39).

To see how we may do this, consider initially a general form for the remainder matrix $\langle[T_N]\rangle$ and then consider transformation of this matrix to model rotations about the line of sight. We then obtain the following expression for $\langle[T_N(\theta)]\rangle$:

$$\begin{aligned}\langle[T_N(\theta)]\rangle &= [U_3^R]\langle[T_N]\rangle[U_3^R]^{-1} \\ &= \begin{bmatrix}1 & 0 & 0\\ 0 & \cos 2\theta & \sin 2\theta\\ 0 & -\sin 2\theta & \cos 2\theta\end{bmatrix} \\ &\quad \cdot \begin{bmatrix}2A_0 & C-iD & H+iG\\ C+iD & B_0+B & E+iF\\ H-iG & E-iF & B_0-B\end{bmatrix} \\ &\quad \cdot \begin{bmatrix}1 & 0 & 0\\ 0 & \cos 2\theta & -\sin 2\theta\\ 0 & \sin 2\theta & \cos 2\theta\end{bmatrix}. \end{aligned} \tag{40}$$

The next step is to realize that the coherency matrix $\langle[T_N]\rangle$ will be made up from fluctuations of vectors which lie in some subspace of the total space of all possible target fluctuations. Hence, there will always exist target vectors $\underline{v}$ such that

$$\langle[T_N]\rangle\underline{v} = 0 \Rightarrow \langle[T_N(\theta)]\rangle\underline{v} = 0. \tag{41}$$

The vectors $\underline{v}$ define the null space of the N-target. The requirement for invariance under rotations then means that the null space $\underline{v}$ should be unchanged under the transformation of (40) (as shown on the right of (41)). Mathematically, this requirement is equivalent to stipulating that the single target $[T_s]$ contains all the components from target vectors which lie in the null space of the N-target and that this null space does not change under rotation.

By substituting (40) into (41), it is easy to show that in order to satisfy both these constraints, the vectors $\underline{v}$ must be the eigenvectors of the rotation matrix $[U_3^R]$ as shown in (42) (these ideas were originally presented in [17])

$$\begin{aligned}&\langle[T_N(\theta)]\rangle\underline{v} = 0 \Rightarrow \\ &([U_3^R]^{-1} - \lambda I_3)\underline{v} = 0.\end{aligned} \tag{42}$$

It then follows that there are three principal Huynen type decompositions, generated by the 3 eigenvectors in (42), i.e., $\underline{v}_1 = (1, 0, 0)^T$, $\underline{v}_2 = (1/\sqrt{2})(0, 1, i)^T$, and $\underline{v}_3 = (1/\sqrt{2})(0, 1, -i)^T$. The decomposition described in (39) is generated by using the first eigenvector $\underline{v}_1$ as the null space. The choice of this eigenvector means that the N-target must have zeros across the first column and row of its coherency matrix, as shown in (39). The other two eigenvectors $\underline{v}_2$ and $\underline{v}_3$ are associated with helical type scattering and give rise to remainder matrices which also satisfy the constraint of null space invariance under rotations.

Huynen has stated [18], [19] that although mathematically there are three such decompositions, the first eigenvector $\underline{v}_1$ is always to be selected on physical grounds, since its space is associated with all target components which have $S_{xx} + S_{yy} \neq 0$. Many scatterers such as spheres and smooth surfaces give scattering with components along such directions (which Huynen terms "symmetric" components). Huynen postulates that since such features are commonly part of the underlying average target it makes sense to generate an N-target which has these as a null space.

However, all of this clearly leaves three different decompositions with three completely different rank one coherency matrices for the equivalent single target. Such a situation is not entirely satisfactory. It would be better in fact to find a representation which is independent of *all* unitary transformations of the coherency matrix $\langle[T]\rangle$. As we shall discuss later, eigenvector decompositions present such a set of options.

The fact that the eigenvectors $\underline{v}_1$, $\underline{v}_2$, and $\underline{v}_3$ are invariant under rotations about the line of sight implies that if the coherency matrix for a random medium is to be rotationally invariant (i.e., to yield the same coherency matrix irrespective of rotation angle) then it must be constructed from a linear combination of the outer products of these eigenvectors, i.e.,

$$\begin{aligned}\langle[T]\rangle &= [T_1] + [T_2] + [T_3] \\ &= \alpha\underline{v}_1\underline{v}_1^\dagger + \beta\underline{v}_2\underline{v}_2^\dagger + \gamma\underline{v}_3\underline{v}_3^\dagger \\ &= \begin{bmatrix}\alpha & 0 & 0\\ 0 & \beta+\gamma & i(\beta-\gamma)\\ 0 & -i(\beta-\gamma) & \beta+\gamma\end{bmatrix}.\end{aligned} \tag{43}$$

The eigenvalues of this matrix are $\lambda_1 = \alpha, \lambda_2 = 2\beta$, and $\lambda_3 = 2\gamma$, i.e., it has rank $r \geq 1$ and so represents a distributed or random target. The covariance matrix $[C]$ related to $[T]$ in (43) was first derived by Ngheim *et al.* [20] using a direct expansion of the elements of $[C]$. This eigenvector method provides a shorter and clearer derivation of the same result. Note that for such rotationally symmetric media, the coherency matrix has only 3 independent parameters.

While the rotation matrix $[U_3^R]$ is of special interest, we must also be careful to consider the wider class of transformations obtained by changing the wave polarization basis. While these include rotations, they also extend the possibilities into complex transformations (to obtain left and right circular from linear polarization for example).

We can generate the form of the coherency matrix for arbitrary elliptical polarization as shown in (44), which again represents a unitary similarity transformation where the parameter ρ is the complex polarization ratio describing the change of elliptical polarization base [6], [7], [21]. In this case, the change of polarization base represents a two component unitary transformation as shown in (44):

$$\begin{aligned}[T_{3A}(\rho)] &= [U_3^B][T_{3A}][U_3^B]^{-1} \\ [U_3^B] &= \frac{1}{2(1+\rho\rho^*)} \\ &\quad \cdot \begin{bmatrix}2+\rho^2+\rho^{*2} & \rho^{*2}-\rho^2 & 2(\rho-\rho^*)\\ \rho^2+\rho^{*2} & 2-(\rho^2+\rho^{*2}) & 2(\rho+\rho^*)\\ 2(\rho-\rho^*) & -2(\rho+\rho^*) & 2(1-\rho\rho^*)\end{bmatrix}.\end{aligned} \tag{44}$$

Clearly, the residue N-matrix in the Huynen type decomposition is not invariant under the wider class of transformations represented by (44) (since the eigenvectors of $[U_3^B]$ are no longer $\underline{v}_1\underline{v}_2$ and $\underline{v}_3$). Indeed, we have seen in Section II-D that the Huynen decomposition presupposes that the HH and VV scattering coefficients are always negatively correlated. In general we can expect to observe other types of fluctuations of the target vector and still hope to generate the concept of an average dominant rank one coherency matrix. For this reason, other attempts have been made to formulate the decomposition problem in a more general polarization basis invariant form. We now turn to consider these in more detail.

$$\beta_1 = \begin{pmatrix} 0 & 1 & 0 \\ 1 & 0 & 0 \\ 0 & 0 & 0 \end{pmatrix} \quad \beta_2 = \begin{pmatrix} 0 & -i & 0 \\ i & 0 & 0 \\ 0 & 0 & 0 \end{pmatrix} \quad \beta_3 = \begin{pmatrix} 1 & 0 & 0 \\ 0 & -1 & 0 \\ 0 & 0 & 0 \end{pmatrix}$$

$$\beta_4 = \begin{pmatrix} 0 & 0 & 1 \\ 0 & 0 & 0 \\ 1 & 0 & 0 \end{pmatrix} \quad \beta_5 = \begin{pmatrix} 0 & 0 & -i \\ 0 & 0 & 0 \\ i & 0 & 0 \end{pmatrix} \quad \beta_6 = \begin{pmatrix} 0 & 0 & 0 \\ 0 & 0 & 1 \\ 0 & 1 & 0 \end{pmatrix}$$

$$\beta_7 = \begin{pmatrix} 0 & 0 & 0 \\ 0 & 0 & -i \\ 0 & i & 0 \end{pmatrix} \quad \beta_8 = \frac{1}{\sqrt{3}} \begin{pmatrix} 1 & 0 & 0 \\ 0 & 1 & 0 \\ 0 & 0 & -2 \end{pmatrix}$$

Fig. 4. The 8 Gell–Mann matrices for parameterization of 3 × 3 Unitary matrices.

IV. Eigenvector-Based Decompositions

A second class of TD theorems are those based on eigenvalues of the coherency matrix. Since the eigenvalue problem is automatically basis invariant, such decompositions have been suggested as alternatives to the Huynen approach. Further, since they can be used to generate a diagonal form of the coherency matrix which we can physically interpret as statistical independence between a set of target vectors, then such an approach might be expected to yield a general decomposition into independent scattering processes.

According to this method, we write the coherency matrix in the form of (45)

$$\langle [T] \rangle = [U_3][\Sigma][U_3]^{-1} \tag{45}$$

where $[\Sigma]$ is a 3 × 3 diagonal matrix with nonnegative real elements. Cloude was first to consider such a decomposition [16], [22], based on an algorithm to identify the dominant scattering mechanism via extraction of the largest eigenvalue, while Holm [23] provided an alternative physical interpretation of the covariance eigenvalue spectrum (46):

$$\begin{aligned} [\Sigma] &= \begin{bmatrix} \lambda_1 & 0 & 0 \\ 0 & \lambda_2 & 0 \\ 0 & 0 & \lambda_3 \end{bmatrix}_{\lambda_1 \geq \lambda_2 \geq \lambda_3} \\ &= \begin{bmatrix} \lambda_1 - \lambda_2 & 0 & 0 \\ 0 & 0 & 0 \\ 0 & 0 & 0 \end{bmatrix} + \begin{bmatrix} \lambda_2 - \lambda_3 & 0 & 0 \\ 0 & \lambda_2 - \lambda_3 & 0 \\ 0 & 0 & 0 \end{bmatrix} \\ &\quad + \begin{bmatrix} \lambda_3 & 0 & 0 \\ 0 & \lambda_3 & 0 \\ 0 & 0 & \lambda_3 \end{bmatrix}. \end{aligned} \tag{46}$$

He interpreted the target as a sum of a single $[S]$ matrix (rank 1 coherency matrix) plus two noise or remainder terms. This is a hybrid approach, combining an eigenvalue analysis (providing invariance under unitary transformations) with the concept of the single target plus noise model of the Huynen approach.

The basic idea of the eigenvector approach is to represent $[M]$ as the sum of three components, where *each* matrix $[M_i]$ corresponds to a scattering matrix $[S_i]$. The physical basis for choosing the target components is to establish statistical independence between the targets $[S_i]$. This approach has also been used to generate statistically independent images for speckle reduction through multipolarization averaging (the polarization whitening filter [24]). The eigenvector method has also been used as part of the radar calibration problem [25].

There is one potential problem with such an approach: The unitary matrix $[U_3]$ in (45) is a generalized version of that used in (44). It is an 8-parameter complex matrix. This observation leads to some difficulties in relating the eigenvalues of $[T]$ to the radar cross section optimization problem [26]. In this case, the eigenvalues of $[T]$ provide only loose bounds on the variability of radar cross section of a target with polarization agility. Consequently, the maximum variation of RCS will generally be less than rather than equal to the ratio of maximum and minimum eigenvalues of $[T]$.

However, for TD theorems, we are not concerned with the radar cross section problem since it involves the antenna polarization state. In TD theorems, we are concerned only with properties of the target itself and not the antenna states. It can be shown that the general 3 × 3 unitary matrix $[U_3]$ can be parameterize in terms of 8 angles $\underline{w}$ as the matrix exponential of a Hermitian matrix constructed from the Gell–Mann basis matrix set $\underline{\beta}$ (47) [27]:

$$\begin{aligned} \langle [T(\underline{w})] \rangle &= [U_3] \langle [T] \rangle [U_3]^{-1} \\ &= \exp(i\underline{w}.\underline{\beta}) \langle [T] \rangle \exp(-i\underline{w}.\underline{\beta}) \\ &= \sum_{j=1}^{3} \lambda_j \underline{e}_j \underline{e}_j^{\dagger} \\ [U_3] &= [\underline{e}_1 \quad \underline{e}_2 \quad \underline{e}_3] \end{aligned} \tag{47}$$

where $\underline{w}$ is a real 8-element vector and the matrices $\underline{\beta}$ represent the set of 8 Gell–Mann matrices shown in Fig. 4. The vectors $\underline{e}_j$ are the eigenvectors of $\langle [T] \rangle$. Note that although a 3 × 3 unitary matrix has 8 parameters, two of them (β_3 and β_8) are unobservable in measured coherency matrices since the latter is generated from a quadratic product of conjugate matrix factors. These two matrices form a special algebra, called the Cartan subalgebra, which can be used to classify general unitary transformations [27]. For nonreciprocal scattering, when $[S]$ cannot be assumed symmetric, use must be made of the 15 modified Dirac matrices to parameterize the set of 4 × 4 unitary matrices [27]. In this case the unobservable Cartan subalgebra is 3 dimensional, leaving parameterization in terms of 4 eigenvalues and 12 angles. Fortunately, however,

for most radar problems of interest, the representation of (47) is adequate.

This approach to TD theorems provides a representation of the target in terms of 9 real elements: the three nonnegative eigenvalues of the coherency matrix and a set of 6 angles which represent the triple of independent rank-1 target components. The eigenvalues can be interpreted as weights for these various target components.

An advantage of using the eigenvector representation is that it provides a formal connection with signal processing theory so that for example we can subtract any noise eigenvalues obtained from known or estimated system noise in the covariance matrix estimation problem. Such noise will be basis invariant and so have a coherency matrix of the general form shown in (48)

$$\langle [T_{\text{noise}}] \rangle = \sigma \begin{bmatrix} 1 & 0 & 0 & 0 \\ 0 & 1 & 0 & 0 \\ 0 & 0 & 1 & 0 \\ 0 & 0 & 0 & 1 \end{bmatrix}. \tag{48}$$

Consequently, noise filtering can be achieved by simple subtraction of σ from the eigenvalues of $\langle [T] \rangle$.

Very often, we are not so concerned with the absolute value of the eigenvalues but rather in their ratios, in which case we calculate the target entropy H (defined in the Von Neumann sense [52]) from the logarithmic sum of eigenvalues of $[T]$ (49)

$$H = \sum_{i=1}^{n} -P_i \log_n P_i \quad P_i = \frac{\lambda_i}{\sum_{j=1}^{n} \lambda_j} \tag{49}$$

where $n = 3$ for backscatter problems and $n = 4$ for bistatic scattering. In general we arrange that the entropy is a scalar measure with range $0 \leq H \leq 1$. The entropy of polarized wave states in random media has been extensively studied in [52]. Here, however, we consider the entropy of the scattering medium, not of the wave itself.

If the entropy H is low then the system may be considered weakly depolarizing and we can extract the dominant target scattering matrix component as the eigenvector corresponding to the largest eigenvalue and ignore the other eigenvector components [50], [51]. It can be shown that this vector corresponds to a least-squares estimate of the underlying dominant single scattering matrix for the target [29]. Such low entropy scattering has recently been used to examine details of multiple scattering phenomena in low loss media [30]. Examples of low entropy targets are provided by surface scattering from smooth sea ice, lava flows, and the ocean surface, but also for backscatter from some types of crop species in vegetation mapping applications where, despite averaging over surface and volume statistics, the polarization ratios remain constant, leading to a rank one coherency matrix (see Section VII).

If the entropy is high then the target is depolarizing and we can no longer consider it as having a single equivalent scattering matrix and we must consider the full eigenvalue spectrum. Further, as the entropy increases, the number of distinguishable classes identifiable from polarimetric observations is reduced [31]. In the limit $H = 1$, the polarization information becomes zero and the target scattering is truly a random noise process (at least up to second order statistics). In such cases it may be necessary to resort to higher order statistics or multifrequency information for target discrimination.

However, it is important to note that many random distributed natural targets have an entropy significantly less than one. This somewhat surprising observation has lead to increased interest in the use of polarization for the extraction of important average physical properties such as forest biomass [36]–[38].

The general radar target is now represented in terms of 9 parameters: the 3 eigenvalues λ_1, λ_2, λ_3, and a 6-element vector $\underline{w}$. In applications, one or more of these parameters may be zero and so we can reduce the dimensionality of the problem. However, the above procedure provides the most general framework, assuming only reciprocity and linearity.

In summary, we have seen that there are two options for the basis invariant treatment of polarimetric data: the first to extract the dominant eigenvector of $\langle [T] \rangle$ and the second to consider the complete triple of independent target vectors represented by the phase vector $\underline{w}$. We shall see that for targets with reflection symmetry, these two methods become entirely equivalent (see (63)).

V. Model-Based Decompositions

As an important example of the application of unitary transformations to a high entropy problem, consider generation of the coherency matrix for single scattering from a cloud of identical particles with random orientations. In this instance we postulate that each particle in the cloud has a backscatter matrix of the form

$$[S] = \begin{bmatrix} a & 0 \\ 0 & d \end{bmatrix} \tag{50}$$

where a and d are complex scattering coefficients in the particle characteristic coordinate system. In this case we can generate the effect of rotation about the line of sight as

$$\begin{aligned} [T_3(\theta)] &= \begin{bmatrix} 1 & 0 & 0 \\ 0 & \cos 2\theta & -\sin 2\theta \\ 0 & \sin 2\theta & \cos 2\theta \end{bmatrix} \begin{bmatrix} \alpha & \beta & 0 \\ \beta^* & \delta & 0 \\ 0 & 0 & 0 \end{bmatrix} \\ &\quad \cdot \begin{bmatrix} 1 & 0 & 0 \\ 0 & \cos 2\theta & \sin 2\theta \\ 0 & -\sin 2\theta & \cos 2\theta \end{bmatrix} \\ &= \begin{bmatrix} \alpha & \beta \cos 2\theta & \beta \sin 2\theta \\ \beta^* \cos 2\theta & \delta \cos^2 2\theta & \delta \sin 2\theta \cos 2\theta \\ \beta^* \sin 2\theta & \delta \sin 2\theta \cos 2\theta & \delta \sin^2 2\theta \end{bmatrix} \end{aligned} \tag{51}$$

where $\alpha = |(a+d)|^2/2$, $\delta = |(a-d)|^2/2$, and $\beta = (a+d)(a^*-d^*)/2$. If we now average over all angles θ then

we obtain a form of the coherency matrix as shown in (52)

$$\langle [T_3(\theta)] \rangle = \tfrac{1}{2} \begin{bmatrix} 2\alpha & 0 & 0 \\ 0 & \delta & 0 \\ 0 & 0 & \delta \end{bmatrix}. \tag{52}$$

We see that in this problem the Pauli matrix basis generates a diagonal coherency matrix and so the Pauli matrices are the eigenstates for this system (note that the system does not have a single equivalent $[S_A]$ matrix representation). The entropy of this system is easily evaluated as

$$H = -\left\{ \frac{\alpha}{(\alpha+\delta)} \log_3 \left[\frac{\alpha}{(\alpha+\delta)} \right] + \frac{\delta}{(\alpha+\delta)} \log_3 \left[\frac{\delta}{2(\alpha+\delta)} \right] \right\} \tag{53}$$

and the matrix $[U]$ is simply the 3×3 identity matrix so the vector $\underline{w} = \underline{0}$. Note that the covariance matrix $[C]$ has the same eigenvalues but the corresponding general form

$$[C] = \tfrac{1}{2} \begin{bmatrix} 2\alpha+\delta & 0 & 2\alpha-\delta \\ 0 & 2\delta & 0 \\ 2\alpha-\delta & 0 & 2\alpha+\delta \end{bmatrix} \tag{54}$$

from which it follows that the copolar scattering coefficients are uncorrelated with the crosspolar terms.

Two examples will illustrate the usefulness of these results. If we have a cloud of spheres then $a = d$ and $\delta = 0$, leading to $H = 0$, i.e., a zero entropy system. In this case, averaging over orientation makes no change to the polarimetric response, due to the symmetry of the sphere. Hence, despite having a random scattering problem, we observe a zero entropy system! This has important implications for the use of polarization to observe multiple scattering effects [30]. Since the single scattering contributions have $H = 0$, then choice of sphere reject circular polarization will entirely remove the single scattering contributions from observation, leaving only the multiple scattering terms.

At the other extreme, consider a cloud of needle like particles for which $d = 0$ in (50). In this case $\alpha = \delta$ and the entropy is $H = 0.95$, which represents a strongly depolarizing system. This result has been used in radar remote sensing observations of scattering from mature forests (the Freeman decomposition [32], [33]), where the distinct polarimetric signature ($H = 0.95$) of random particle scattering can be used to extract its contribution from the observed matrix response. Note that in this case the covariance matrix (54) has the simplified form

$$[C] = A \begin{bmatrix} 3 & 0 & 1 \\ 0 & 2 & 0 \\ 1 & 0 & 3 \end{bmatrix}. \tag{55}$$

Freeman has considered a decomposition of the covariance matrix which employs this model of random scattering (f_v) together with two rank one scattering processes for slightly rough surfaces (f_s) and dihedral scattering (f_d). His decomposition has the general form [32], [33]

$$\begin{aligned}[C] &= f_v \begin{bmatrix} 1 & 0 & \frac{1}{3} \\ 0 & \frac{2}{3} & 0 \\ \frac{1}{3} & 0 & 1 \end{bmatrix} + f_s \begin{bmatrix} y^2 & 0 & y \\ 0 & 0 & 0 \\ y & 0 & 1 \end{bmatrix} \\ &\quad + f_d \begin{bmatrix} x^2 & 0 & -x \\ 0 & 0 & 0 \\ -x & 0 & 1 \end{bmatrix} \\ &= \begin{bmatrix} f_v + f_d x^2 + f_s y^2 & 0 & \frac{f_v}{3} - x f_d + y f_s \\ 0 & \frac{2f_v}{3} & 0 \\ \frac{f_v}{3} - x f_d + y f_s & 0 & f_v + f_d + f_s \end{bmatrix}. \end{aligned} \tag{56}$$

He then obtains the 5 unknown real coefficients from the 4 observed coherency matrix parameters (by setting either x or y equal to 1, depending on the sign of the off diagonal elements of [C]). Note that there is a scale change in this notation compared to that in the original publication by Freeman. This is due to our definition of target vectors in (20) and (21).

While this decomposition can always be applied, it contains two important assumptions which limit its applicability. The first is that the assumed 3-component scattering model is always applicable and the second that the correlation coefficients $\langle hh\, hv^* \rangle = \langle vv\, hv^* \rangle = 0$.

The first restricts application to a class of scattering problems (Freeman originally intended this model for application to backscatter from earth terrain and forests) and becomes invalid for example if we consider surface scattering with entropy different from zero (see Section VII). The second assumption is more important because it turns out that it is generic to a wide class of scattering problems as we now demonstrate.

A. Symmetries and Zero Correlations: Reflection Symmetry

Consider the general scattering problem shown in Fig. 5. It was first shown by van de Hulst [34] that if we know the scattering matrix $[S]$ for a target through some scattering angle θ, then we can immediately find the form of the scattering matrix for 3 other configurations of the scattering problem. These three "daughter" matrices are shown in Fig. 6 for both the general scattering case and more especially for the case of backscatter. The matrices are obtained by the following geometrical transformations.

1) S_α—Rotation by π about the bisectrix vector $\underline{b}$.
2) S_β—Mirror the problem with respect to the scattering plane AOB.
3) S_γ—Mirror the problem with respect to the bisectrix plane.

Here we are concerned particularly with the case of backscatter for which the scattering plane becomes ill-defined but the bisectrix lies along the direction of incidence. From the right hand side of Fig. 6 we see that there are only two possible forms of the scattering matrix, both symmetric (note that we have used the antenna coordinate system for backscatter).

An interesting result follows if we consider now a distributed target which has reflection symmetry in some plane normal to the line of sight (Fig. 7). Physically this mean that whenever we have a contribution from a point at P, there will

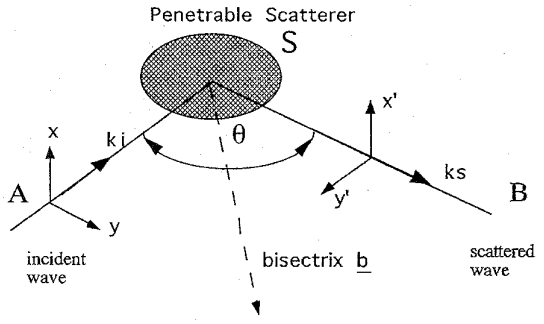

Fig. 5. General vector scattering geometry.

General Transformations

$$S=\begin{pmatrix} a & b \\ c & d \end{pmatrix} \Rightarrow \begin{cases} S_\alpha = \begin{pmatrix} a & -c \\ -b & d \end{pmatrix} \\ S_\beta = \begin{pmatrix} a & -b \\ -c & d \end{pmatrix} \\ S_\gamma = \begin{pmatrix} a & c \\ b & d \end{pmatrix} \end{cases}$$

Backscatter Transformations

$$S_A=\begin{pmatrix} a & b \\ b & d \end{pmatrix} \Rightarrow \begin{cases} S_\alpha = \begin{pmatrix} a & b \\ b & d \end{pmatrix} \\ S_\beta = \begin{pmatrix} a & -b \\ -b & d \end{pmatrix} \\ S_\gamma = \begin{pmatrix} a & -b \\ -b & d \end{pmatrix} \end{cases}$$

Fig. 6. The set of possible scattering matrix transformations.

always be a corresponding contribution from its image at Q, for *some* axis AA'.

However, from Fig. 6 and by adopting the Pauli matrix vectorization of $[S]$, it follows that the two contributions from P and Q will have related target vectors of the form

$$\begin{aligned} \underline{k}_P &= [\alpha \quad \beta \quad \gamma]^T \Rightarrow \\ \underline{k}_Q &= [\alpha \quad \beta \quad -\gamma]^T \end{aligned} \tag{57}$$

and so after integration we obtain two independent components in the composition of the observed coherency matrix as shown schematically in (58)

$$\begin{aligned} \langle [T] \rangle &= \langle [T_1] \rangle + \langle [T_2] \rangle \\ &= \begin{bmatrix} x & x & x \\ x & x & x \\ x & x & x \end{bmatrix} + \begin{bmatrix} x & x & -x \\ x & x & -x \\ -x & -x & x \end{bmatrix} \\ &= \begin{bmatrix} x & x & 0 \\ x & x & 0 \\ 0 & 0 & x \end{bmatrix} \end{aligned} \tag{58}$$

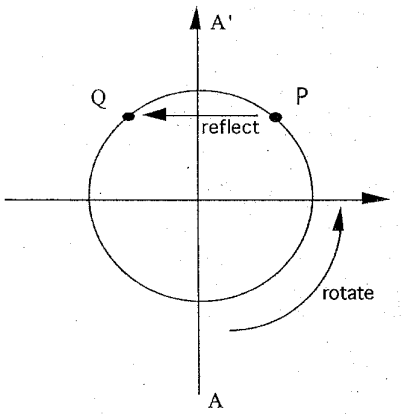

Fig. 7. Reflection symmetry and rotations about the line of sight.

where we have used the symbol x to represent a general nonzero element of $[T]$. This is our main result. It shows that if the scatterer has reflection symmetry in a plane normal to the line of sight then the coherency matrix will have the general form shown on the right in (58), i.e., the crosspolar scattering coefficient will be uncorrelated with the copolar terms. It is easy to show that under these circumstances the covariance matrix has the generic form

$$[C] = \begin{bmatrix} x & 0 & x \\ 0 & x & 0 \\ x & 0 & x \end{bmatrix} \tag{59}$$

which is of the general form used in the Freeman decomposition (56). Under these conditions the coherency matrix has only 5 parameters and the vector $\underline{w}$ reduces in complexity so that we can obtain simple analytic expressions for the eigenvectors and eigenvalues of $[T]$.

Before leaving this section, let us consider the coherency matrix for a medium which exhibits not only reflection symmetry in some special plane but also rotation symmetry, so that all planes in Fig. 7 become valid reflection planes. This type of symmetry is generally referred to as azimuthal symmetry (although in the literature the symmetry of (57) is often loosely described as azimuthal) and we can find the form of the observed coherency matrix by combining (43) and (58) to obtain

$$\begin{aligned} \langle [T] \rangle &= [T_1] + [T_2] \\ &= \begin{bmatrix} \alpha & 0 & 0 \\ 0 & \beta+\gamma & i(\beta-\gamma) \\ 0 & -i(\beta-\gamma) & \beta+\gamma \end{bmatrix} \\ &\quad + \begin{bmatrix} \alpha & 0 & 0 \\ 0 & \beta+\gamma & -i(\beta-\gamma) \\ 0 & i(\beta-\gamma) & \beta+\gamma \end{bmatrix} \\ &= 2 \begin{bmatrix} \alpha & 0 & 0 \\ 0 & \beta+\gamma & 0 \\ 0 & 0 & \beta+\gamma \end{bmatrix} \end{aligned} \tag{60}$$

which has only 2 independent parameters α and β. In this case $\underline{w}$ is the null vector, the Pauli matrices are the eigen-

vectors, and $[T]$ has two equal eigenvalues. Note that the Chandrasekhar decomposition of (6) can be caste in this form for the special but important case of scattering through $\theta = 90°$ [16].

In summary, we have seen that the less restrictive plane reflection symmetry reduces the number of parameters in $[T]$ to 5 and the vector $\underline{w}$ is not in general zero, while true azimuthal symmetry further reduces the number of elements to 2 and yields a diagonal coherency matrix in the Pauli matrix base so that the vector $\underline{w}$ is the null vector.

B. Target Decomposition for Targets with Reflection Symmetry

In this section we consider the special but important case of reflection symmetry when, as follows from (30), the coherency and covariance matrices are related as shown in (61)

$$[T] = \tfrac{1}{2}\begin{bmatrix}1 & 0 & 1\\ 1 & 0 & -1\\ 0 & \sqrt{2} & 0\end{bmatrix}\begin{bmatrix}1 & 0 & \rho\\ 0 & \eta & 0\\ \rho^* & 0 & \zeta\end{bmatrix}\begin{bmatrix}1 & 1 & 0\\ 0 & 0 & \sqrt{2}\\ 1 & -1 & 0\end{bmatrix}$$
$$= \tfrac{1}{2}\begin{bmatrix}1+\zeta+(\rho+\rho^*) & 1-\zeta-(\rho-\rho^*) & 0\\ 1-\zeta+(\rho-\rho^*) & 1+\zeta-(\rho+\rho^*) & 0\\ 0 & 0 & 2\eta\end{bmatrix}. \quad (61)$$

The first to generate the form of the eigenvector decomposition of this problem [35], [36] was van Zyl. Since the matrix $[T]$ has only two nonzero off diagonal terms, the eigenvalues can be found from a 2×2 submatrix and expressed analytically as shown in (62)

$$[\Sigma] = \tfrac{1}{2}\begin{bmatrix}1+\zeta+\sqrt{\Delta} & 0 & 0\\ 0 & 1+\zeta-\sqrt{\Delta} & 0\\ 0 & 0 & 2\eta\end{bmatrix}$$
$$\Delta = (\zeta-1)^2 + 4\rho\rho^*. \quad (62)$$

The three eigenvectors can likewise be parameterize in the form of a unitary matrix as shown in (63)

$$[U_3] = \begin{bmatrix}e^{i\phi}\cos\alpha & e^{i\delta}\sin\alpha & 0\\ -e^{-i\delta}\sin\alpha & e^{-i\phi}\cos\alpha & 0\\ 0 & 0 & 1\end{bmatrix} \quad (63)$$

for which the vector $\underline{w}$ has the general form

$$\underline{w} = [w_i \quad w_2 \quad w_3 \quad 0 \quad 0 \quad 0 \quad 0 \quad 0]. \quad (64)$$

Note that the unitary matrix can in this case be written in a simplified form as

$$[U_3] = \begin{bmatrix}U_2 & 0\\ 0 & 1\end{bmatrix} \Rightarrow$$
$$[U_2] = \exp(i\Omega\underline{\sigma}.\underline{n})$$
$$= \cos\Omega + i\sin\Omega\underline{\sigma}.\underline{n} \quad (65)$$

which represents a rotation in R_3 through an angle $\Omega = |\underline{w}|$ about an axis with direction vector $\underline{n} = (1/|\underline{w}|)[w_1 \quad w_2 \quad w_3]$. The backscatter from terrain with such reflection symmetry can then be classified by 5 parameters: the three eigenvalues of $[T]$ and any one of the sets (α, δ, ϕ), (w_1, w_2, w_3), or (Ω, n_1, n_2, n_3). Note that the Cartan subalgebra for this problem is 1 dimensional (the phase angle ϕ is not observable from the coherency matrix).

To see this, note that we can write the coherency matrix directly in terms of these parameters (see (66) shown at the bottom of the page) from which we see that the phase angles in the unitary transformation depend on the phase angle of the correlation between two target vector components. The angle α, on the other hand, depends on the dominant scattering mechanism, ranging from 0° for surface scattering under the stationary phase or geometrical optics approximation through 45° for linear dipole scattering to 90° for dihedral scatter.

Note that for terrain with this symmetry, we effectively have only one *independent* scattering mechanism (that determined by the largest eigenvalue). This considerably simplifies the physical interpretation of random polarimetric scattering from symmetric media, since we need only consider one scattering mechanism and its entropy or degree of randomness.

We can also calculate the form of the covariance matrix $[C]$ for such media in terms of the invariant parameters to obtain (67), shown at the bottom of the page. This form of the covariance matrix is very interesting. It shows that, for example, the correlation coefficient between hh and vv is a function of *both* the eigenvalue spectrum (the entropy of the scattering process) and the angle α (the type of scattering process). This can make it difficult to use this parameter for identification of scattering mechanisms in radar imagery. As a simple example, for dipole scattering where $|hh| \gg |vv|$ and $\alpha = 45°$, the correlation will always be small but the entropy can still be zero, i.e., we can have a strongly polarized scattering problem with an apparently low value of correlation. All of this again points us toward

$$\langle[T]\rangle = \begin{bmatrix}e^{i\phi}\cos\alpha & e^{i\delta}\sin\alpha & 0\\ -e^{-i\delta}\sin\alpha & e^{-i\phi}\cos\alpha & 0\\ 0 & 0 & 1\end{bmatrix}\begin{bmatrix}\lambda_1 & 0 & 0\\ 0 & \lambda_2 & 0\\ 0 & 0 & \lambda_3\end{bmatrix}\begin{bmatrix}e^{-i\phi}\cos\alpha & -e^{i\delta}\sin\alpha & 0\\ e^{-i\delta}\sin\alpha & e^{i\phi}\cos\alpha & 0\\ 0 & 0 & 1\end{bmatrix}$$
$$= \begin{bmatrix}\lambda_1\cos^2\alpha + \lambda_2\sin^2\alpha & \cos\alpha\sin\alpha(\lambda_2-\lambda_1)e^{i(\delta+\phi)} & 0\\ \cos\alpha\sin\alpha(\lambda_2-\lambda_1)e^{-i(\delta+\phi)} & \lambda_2\cos^2\alpha + \lambda_1\sin^2\alpha & 0\\ 0 & 0 & \lambda_3\end{bmatrix}. \quad (66)$$

$$\langle[C]\rangle = \begin{bmatrix}(\lambda_1+\lambda_2) + 2(\lambda_1-\lambda_2)\sin 2\alpha\cos\delta & 0 & (\lambda_1-\lambda_2)(\cos 2\alpha + i\sin 2\alpha\sin\delta)\\ 0 & 2\lambda_3 & 0\\ (\lambda_1-\lambda_2)(\cos 2\alpha - i\sin 2\alpha\sin\delta) & 0 & (\lambda_1+\lambda_2) - 2(\lambda_1-\lambda_2)\sin 2\alpha\cos\delta\end{bmatrix}. \quad (67)$$

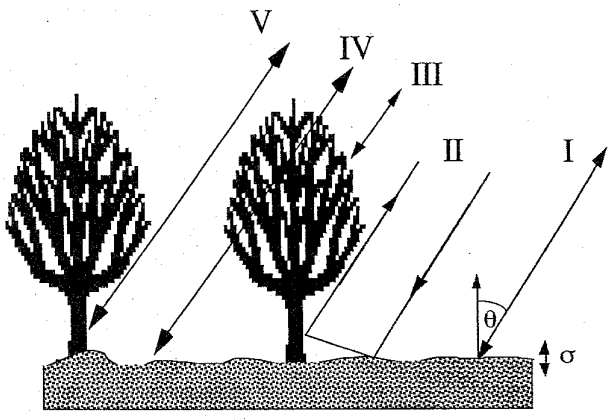

Fig. 8. Five important scattering mechanisms in radar remote sensing.

use of the invariant eigenvalue/eigenvector parameters for the interpretation of POLSAR imagery.

VI. Polarimetric Terrain Scattering Models

As first pointed out by van Zyl [35], the first two columns of (63) represent rank one scattering processes with zero linear cross polarization and a relative phase angle of 180° between the columns. He suggested a physical interpretation of these columns in terms of odd and even multiple scattering mechanisms. It is instructive to examine the basis for this interpretation and discover which of the alternative representations of $[U_3]$ yield the best physical insight.

We can identify at least five important scattering mechanisms in radar remote sensing (Fig. 8):

I) backscattering from a rough surface;
II) low-order multiple scattering, as occurs from dihedral effects in forest and urban areas;
III) random volume backscatter from a nonpenetrable layer of discrete scatterers;
IV) surface scattering *after* propagation through a random medium, as occurs in the use of low frequency P- or L-band radar for penetration of vegetation cover;
V) single scattering from anisotropic structures such as tree trunks, where the backscatter can be modeled as that from a rough dielectric cylinder or other canonical object with polarization anisotropy due to shape and dielectric material structure.

Although there are some situations where other scattering mechanisms become important (such as in the radar observation of sea ice where anisotropic propagation and refraction effects can occur [39]), these five provide the basis for the interpretation of many remote sensing scattering problems [34], [35]. The solution of Maxwell's equations for polarization dependent backscatter from such structures is difficult to obtain in general, but the following special cases have been widely used in the literature:

1) Scattering Type I—Surface Scatter Using the Small Perturbation or Bragg Surface Model: The details of this method may be found in [4] and here we note only that it is applicable when the surface roughness is restricted such that the rms surface roughness σ is much smaller than a wavelength (typically $\sigma/\lambda \leq 0.05$). Of course many natural surfaces do not satisfy this relation, even at the longer radar wavelengths, but the simplicity of the solution for this model makes it a popular starting point for analyses. In fact, to first order, this scattering problem has zero entropy and the scattering matrix for the surface (to be called a Bragg surface) has the following general form

$$[S_{\mathrm{I}}] = A \begin{bmatrix} \alpha_{HH} & 0 \\ 0 & \alpha_{VV} \end{bmatrix} \tag{68}$$

where the matrix is expressed in the linearly polarized s (H or TE polarized) and p (V or TM polarized) coordinates, i.e., perpendicular and parallel to the plane of incidence. We see that to first order there is no linear depolarization from a Bragg surface but that in general, $HH \neq VV$. In fact, the coefficients are functions of the average angle of incidence θ and complex relative permittivity ε_r of the surface such that [4]

$$\begin{aligned} \alpha_{HH} &= R_{H1} \\ \alpha_{VV} &= \frac{(\varepsilon_r - 1)[\sin^2\theta - \varepsilon_r(1 + \sin^2\theta)]}{(\varepsilon_r \cos\theta + \sqrt{\varepsilon_r - \sin^2\theta})^2} \end{aligned} \tag{69}$$

where R_{H1} is the Fresnel coefficient for a flat surface (see (72)). Note that we are using the antenna coordinates to represent the elements of this scattering matrix.

We have seen in (63) that in observation of the target coherency matrix, we can extract a dominant eigenvector which has two important parameters: α and δ, such that we can write an equivalent scattering matrix for low entropy targets with reflection symmetry in the form

$$[S_A] = \sqrt{\lambda} \begin{bmatrix} \cos\alpha + \sin\alpha e^{i\delta} & 0 \\ 0 & \cos\alpha - \sin\alpha e^{i\delta} \end{bmatrix}. \tag{70}$$

It is instructive to calculate the values of these two parameters as a function of angle of incidence for backscatter from a slightly rough surface.

Fig. 9 shows that a increases nearly linearly with increasing angle of incidence on the surface. This suggests that measurement may be useful for remotely establishing the local angle of incidence. We shall see in Section IX that such smooth variations in α are indeed observed for SAR geometries where there exists considerable variation of angle of incidence across the image.

Note that for a Bragg surface, the angle δ is practically constant with angle of incidence. This angle is basically a measure of the relative magnitudes of the HH and VV scattering matrix terms: if $|VV| > |HH|$ then $\delta = \pi$ (as in Fig. 10) while if $|HH| > |VV|$ then $\delta = 0$. Since Bragg scattering has $|VV| > |HH|$ then it follows that δ will always be close to π for a Bragg surface (even in the case of complex dielectric constant).

2) Scattering Type II—Low Order Multiple Scattering: In this case we use the fact that the scattering matrix for a multiple event is given by the product of matrices for each event. If we consider simple double interactions (without rotational symmetry) and assume the interactions are quasispecular from Type I surfaces then the scattering problem is again zero

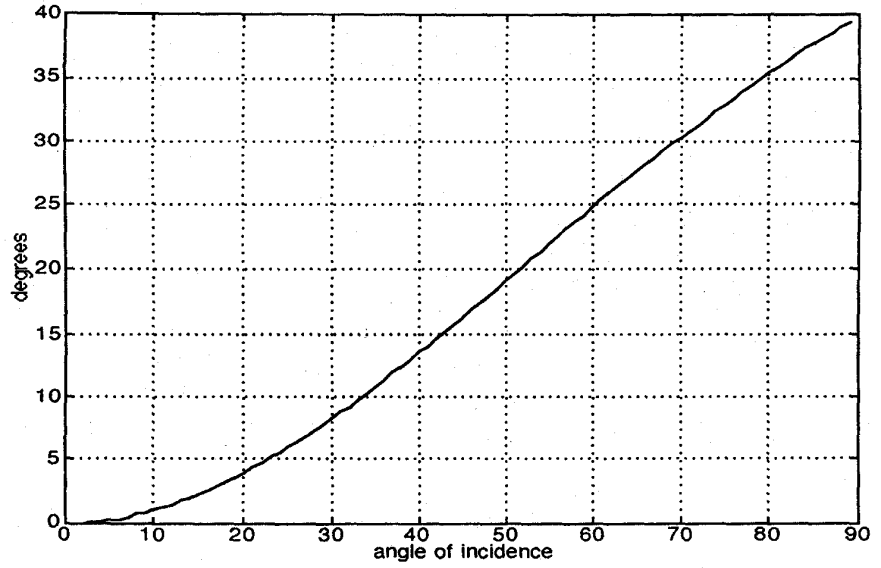

Fig. 9. Alpha variation as a function of angle of incidence for a Bragg surface with $\varepsilon_r = 6 + i0.5$.

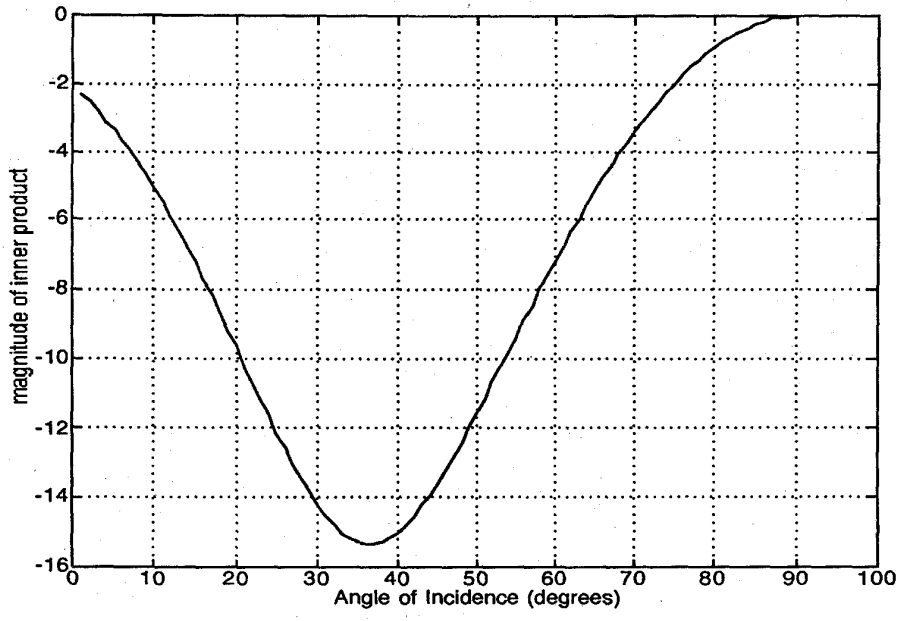

Fig. 10. Inner product between scattering mechanisms I and II, in Fig. 8.

entropy with a scattering matrix

$$[S_{\text{II}}] = \begin{bmatrix} R_{H1}R_{H2} & 0 \\ 0 & -R_{V1}R_{V2} \end{bmatrix} \tag{71}$$

where the R terms are Fresnel coefficients for reflections from surfaces 1 and 2 such that

$$R_{H1} = \frac{\cos\theta - \sqrt{\varepsilon_{r1} - \sin^2\theta}}{\cos\theta + \sqrt{\varepsilon_{r1} - \sin^2\theta}}$$
$$R_{H2} = \frac{\sin\theta - \sqrt{\varepsilon_{r2} - \cos^2\theta}}{\sin\theta + \sqrt{\varepsilon_{r2} - \cos^2\theta}}$$
$$R_{V1} = \frac{\varepsilon_{r1}\cos\theta - \sqrt{\varepsilon_{r1} - \sin^2\theta}}{\varepsilon_{r1}\cos\theta + \sqrt{\varepsilon_{r1} - \sin^2\theta}}$$
$$R_{V2} = \frac{\varepsilon_{r2}\sin\theta - \sqrt{\varepsilon_{r2} - \cos^2\theta}}{\varepsilon_{r2}\sin\theta + \sqrt{\varepsilon_{r2} - \cos^2\theta}}. \tag{72}$$

Note again that use has been made of the antenna coordinates so that phase angles may be directly compared with those for type I scattering.

It is reasonable to assume that the two processes I and II are statistically independent and so the observed coherency matrix is formed from the sum of the two constituent coherency matrices. It is important to note that if we are to be able to separate these two processes as eigenvectors of the observed

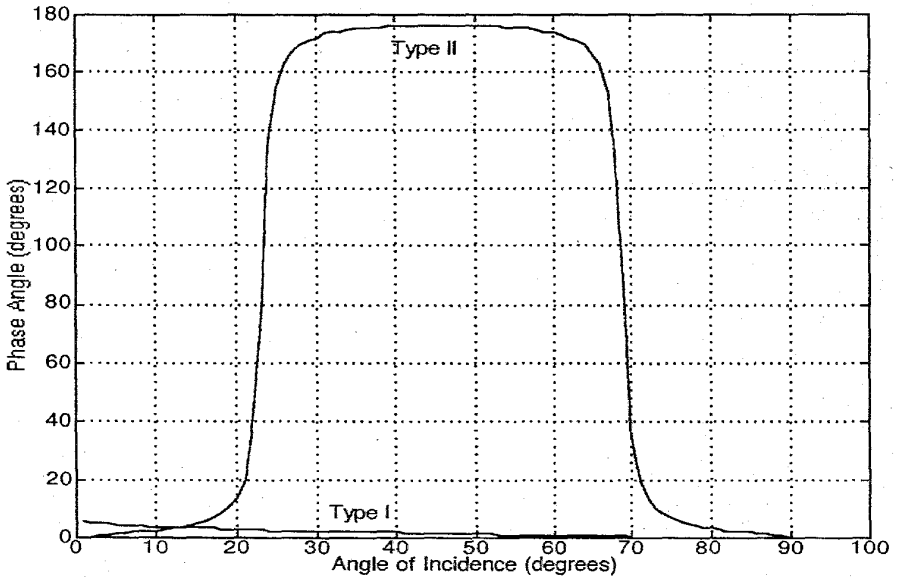

Fig. 11. Phase angle between HH and VV for scattering mechanisms I and II, in Fig. 8.

coherency matrix, then the matrices $[S_{\mathrm{I}}]$ and $[S_{\mathrm{II}}]$ should have orthogonal target vectors $\underline{k}_{\mathrm{I}}$ and $\underline{k}_{\mathrm{II}}$.

It turns out that such an orthogonality condition arises for a wide range of surface types and illumination geometries. To show this, we can generate the following scalar, generated from a complex inner product of normalized target vectors and defined as

$$\kappa = \underline{k}_{\mathrm{I}}^{*T}\underline{k}_{\mathrm{II}} = \frac{|R_{H1}|^2 R_{H2} - R_{V1}R_{V2}\alpha_{VV}^*}{\sqrt{|R_{H1}R_{H2}|^2 + |R_{V1}R_{V2}|^2}.\sqrt{|R_{H1}|^2 + |\alpha_{VV}|^2}}$$
$$0 \le |\kappa| \le 1. \tag{73}$$

Fig. 10 shows a plot of the logarithm of the magnitude of κ as a function of angle of incidence for typical values $\varepsilon_{r1} = \varepsilon_{r2} = 6 + i0.5$. Note that for a wide range of angles around 45° incidence, the two components are nearly orthogonal.

This result has been exploited in the identification of dominant scattering mechanisms in remote sensing from forests [37], [38]. Fig. 11 shows that the phase angle between HH and VV is close to π over a wide range of angles of incidence. As we showed in (63), the eigenvectors of the coherency matrix for symmetric media have π phase difference. In this case, we can associate the amplitude of each scattering component with the eigenvalues of the coherency matrix.

Note, however, that for very small and very large values of θ (the exact values depending on the Brewster angle), the two components are no longer separable in the observed coherency matrix. In these regions, therefore, care must be exercised when interpreting the decomposition of the coherency matrix.

3) Scattering Types III and IV—High Entropy Scattering: The next two types of scattering mechanism (III and IV) are higher entropy processes and so have no single scattering matrix representation. Type III scattering can be modeled as backscatter from a cloud of randomly oriented anisotropic particles, which yields a coherency matrix of the form shown in (55) and a corresponding maximum entropy of 0.95. Note that this mechanism generates linear cross polarization (which is nonetheless decorrelated with the copolar returns). More importantly, this crosspolar generation has an eigenvector component which is orthogonal to *both* processes I and II and so can be observed directly from observation of the backscattered coherency matrix.

In this case, we are justified in decomposing the coherency matrix into processes I, II, and III, due to the fortunate fact that all three mechanisms are (almost) orthogonal and statistically independent, so that the observed coherency matrix is the sum of constituent matrices.

The fourth scattering mechanism (type IV) provides an interesting modification of these ideas. In this class of scattering we propose that a low entropy process (surface scatter or dihedral scatter) is in some way perturbed by propagation through an anisotropic random media.

The propagation mechanism is physically a combination of scattering and absorption as represented by the extinction matrix in (1). For a cloud of nonspherical scatterers, this matrix is nondiagonal and so some polarization transformations occur within this propagation mechanism of the coherent wave. There are two key possibilities. The first that this transformation is unitary and so the low entropy of the problem is preserved. Alternatively, the propagation could cause an increase in the entropy. In this case we would still observe a dominant eigenvector corresponding to the large surface reflection process but with some modification to the observed entropy. If these transformations represent small perturbations of the low entropy phenomena, then we should still be able to classify the scattering behavior, using some suitable nearest neighbor technique.

4) Scattering Type V—Dielectric Target Scattering: The fifth and final mechanism, scattering by a dielectric cylinder, again provides a zero or low entropy scattering process. The

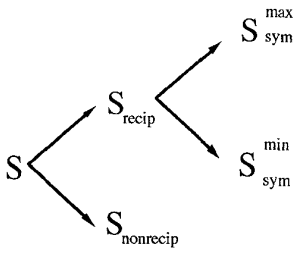

Fig. 12. Cameron decomposition of the coherent scattering matrix.

solution of Maxwell's equations in cylindrical coordinates provides a series representation for polarimetric backscatter from an infinite dielectric cylinder [34]. The convergence of this series depends on the electrical size of the scatterer, and various techniques exist for accelerating the convergence for large cylinders. Here we note only that for normal incidence on such a cylinder the $[S_A]$ matrix is diagonal in the HV base but $HH \neq VV$. However, for oblique incidence, the $[S_A]$ matrix is no longer diagonal in the HV base. The observability of such scattering in the far field coherency matrix will depend on its amplitude and orthogonality with any other independent scattering processes that may be present.

VII. Coherent Decomposition Theorems

A third class of TD theorems are coherent decomposition theorems where the $[S]$ matrix is expressed as the complex sum of basis matrices such as the Pauli matrices used in the vectorization V of (8). In this approach, we associate with each basis matrix an elementary scattering mechanism so that

$$\begin{aligned}[S] &= \begin{bmatrix} a+b & c-id \\ c+id & a-b \end{bmatrix} \\ &= a\begin{bmatrix} 1 & 0 \\ 0 & 1 \end{bmatrix} + b\begin{bmatrix} 1 & 0 \\ 0 & -1 \end{bmatrix} \\ &\quad + c\begin{bmatrix} 0 & 1 \\ 1 & 0 \end{bmatrix} + d\begin{bmatrix} 0 & -i \\ i & 0 \end{bmatrix} \end{aligned} \tag{74}$$

where a, b, c, and d are all complex. In Section II, we showed that such a decomposition is useful as an orthonormal basis for the generation of a target vector from which second order statistics may be defined.

However, an alternative interpretation is to consider application of (74) to deterministic targets, in which case the above decomposition may be considered the coherent composition of four scattering mechanisms: the first being single scattering from a plane surface, the second and third being diplane scattering from corners with a relative orientation of 45°, and the final element being all the antisymmetric components of the matrix $[S]$ (which corresponds to a scatterer which transforms every incident polarization into its orthogonal state). These interpretations are based on consideration of the properties of the Pauli matrices when they undergo a change of wave polarization base.

As two other examples of such an approach to coherent TD, we refer to the work of Krogager [40]–[43] and Cameron [44], [45] who propose specific but very different linear combinations of $[S]$. In the Krogager approach, a symmetric $[S_A]$ matrix is decomposed into three coherent components, which have physical interpretation in terms of diplane, sphere, and helical targets (75)

$$[S] = \alpha[S]_{\text{sphere}} + e^{i\phi}\mu[S]_{\text{diplane}} + e^{i\phi}\eta[S]_{\text{helix}}. \tag{75}$$

This analysis is applied directly to complex $[S]$ matrix imagery and results in characterisation in terms of three images; one for each of the sphere, diplane, and helix responses. A resulting color composite can then be constructed to classify pixels on the basis of the relative contributions of these three mechanisms. Imagery presented using this decomposition displays some interesting structure as shown in [42] and [44].

We can motivate the form of this decomposition by reference to the discussion of rotation invariance in (43). The general form of a coherent role invariant decomposition must be obtained from a linear combination of the eigenvectors of the rotation operator so that

$$\begin{aligned}\underline{k} &= x\begin{pmatrix} 1 \\ 0 \\ 0 \end{pmatrix} + y\begin{pmatrix} 0 \\ 1 \\ i \end{pmatrix} + z\begin{pmatrix} 0 \\ 1 \\ -i \end{pmatrix} \\ &= f\begin{pmatrix} 1 \\ 0 \\ 0 \end{pmatrix} + ge^{i\theta}\begin{pmatrix} 1 \\ 0 \\ i \end{pmatrix} + he^{-i\theta}\begin{pmatrix} 0 \\ 1 \\ -i \end{pmatrix} \end{aligned} \tag{76}$$

where the equality follows from the form of the eigenvalues of the operator and significantly, the scalars f, g, and h are real quantities whereas x, y, and z are complex. Notice that physically this decomposition corresponds to the sum of three targets; a sphere and a pair of left and right handed helices. Note also that the basis elements are orthogonal. Krogager further manipulates this decomposition to incorporate the θ angle inside the target vectors to obtain (77)

$$\underline{k} = f\begin{pmatrix} 1 \\ 0 \\ 0 \end{pmatrix} + (g+h)\begin{pmatrix} 0 \\ e^{i\theta} \\ ie^{i\theta} \end{pmatrix} - 2ih\begin{pmatrix} 0 \\ \sin\theta \\ \cos\theta \end{pmatrix} \tag{77}$$

which yields 3 real coefficients f, g, and h and represents a triple of targets, a sphere, a helix, and a dihedral with orientation θ. However, note that the price to pay for this is that we have lost the orthogonality of target components and, in its original formulation, the elements of the decomposition were not basis invariant.

In the Cameron approach, the $[S_A]$ matrix is decomposed, again using the Pauli matrices, in terms of basis invariant target features (78). Cameron associates importance to a class of targets termed symmetric, which have linear eigenpolarizations on the Poincaré sphere [6], [21] and have a restricted target vector parameterisation. We can represent this decomposition diagrammatically as shown in Fig. 12 and in mathematical form in (78):

$$S = a\cos\theta[\cos\tau S_{\text{sym}}^{\max} + \sin\tau S_{\text{sym}}^{\min}] + \sin\theta S_{\text{nonrecip}}. \tag{78}$$

The first stage is to decompose $[S]$ into reciprocal and nonreciprocal components (by projecting the matrix $[S]$ onto the Pauli matrices and separating the symmetric and nonsymmetric components of the matrix via the angle θ in (78)). The second stage then considers decomposition of the reciprocal term (the

Fig. 13. Entropy image of L-band Flevoland AIRSAR data.

coefficient of $\cos\theta$) into two further components, both of which have linear eigenpolarizations and so are symmetric.

Again we can motivate the form of this decomposition by reference to the effect of a rotation on the target vector. If we use the Pauli matrix expansion of (74), then the effect of a rotation is a transformation of the form

$$\begin{pmatrix} a' \\ b' \\ c' \end{pmatrix} = \begin{bmatrix} 1 & 0 & 0 \\ 0 & \cos 2\theta & -\sin 2\theta \\ 0 & \sin 2\theta & \cos 2\theta \end{bmatrix} \begin{pmatrix} a \\ b \\ c \end{pmatrix}. \tag{79}$$

By definition, it then follows that for symmetric targets, we can always find a θ such that $c' = 0$. Hence, for symmetric targets, b and c cannot be independent and must be related as shown in (80):

$$\underline{k} = a\sigma_0 + \varepsilon(\cos\theta\sigma_1 + \sin\theta\sigma_2) \tag{80}$$

by defining a projection operator D which involves projection onto the Pauli matrix σ_0 and onto the composite matrix $\cos(\theta)\sigma_1 + \sin(\theta)\sigma_2$, where θ is chosen such that

$$\tan 2\theta = \frac{bc^* + b^*c}{|b|^2 - |c|^2}. \tag{81}$$

Cameron was able to show that a general coherent matrix $[S_A]$ can be expressed as a linear combination of two symmetric components DS_A and $(I - D)S_A$. One strength of this approach is that the three components are orthogonal and that the minimum symmetric component $(I - D)S_A$ has only one free parameter, its absolute phase angle.

These two examples highlight a major problem with coherent decompositions; there are many ways of decomposing a given $[S]$, and without *a priori* information, it is impossible to apply a unique decomposition.

Such decompositions also ignore the effect of multiplicative noise from speckle, which is generally a serious problem for SAR imagery in remote sensing. Such coherent noise can distort the interpretation of coherent data. According to the multiplicative noise model, the observed coherent target vector k_{obs} is related to the true target vector (in the Ψ_L basis) as [1]

$$\begin{bmatrix} k_0 \\ k_1 \\ k_2 \\ k_3 \end{bmatrix}_{\text{obs}} = \begin{bmatrix} \varepsilon_1 & 0 & 0 & 0 \\ 0 & \varepsilon_2 & 0 & 0 \\ 0 & 0 & \varepsilon_3 & 0 \\ 0 & 0 & 0 & \varepsilon_4 \end{bmatrix} \begin{bmatrix} S_{HH} \\ S_{HV} \\ S_{VH} \\ S_{VV} \end{bmatrix} = [\Psi]\underline{k} \tag{82}$$

where the complex random variables ε_1 to ε_4 are usually assumed to be Gaussian distributed, with zero mean and associated speckle covariance matrix $[\Sigma]$. In general, we must employ some form of speckle reduction to reduce the effect of these complex random multipliers.

To solve this noise problem various mechanisms are available [46], [47] but they generally involve averaging of the data in some way. All such averages are based on second order statistics (which are required to represent the noise).

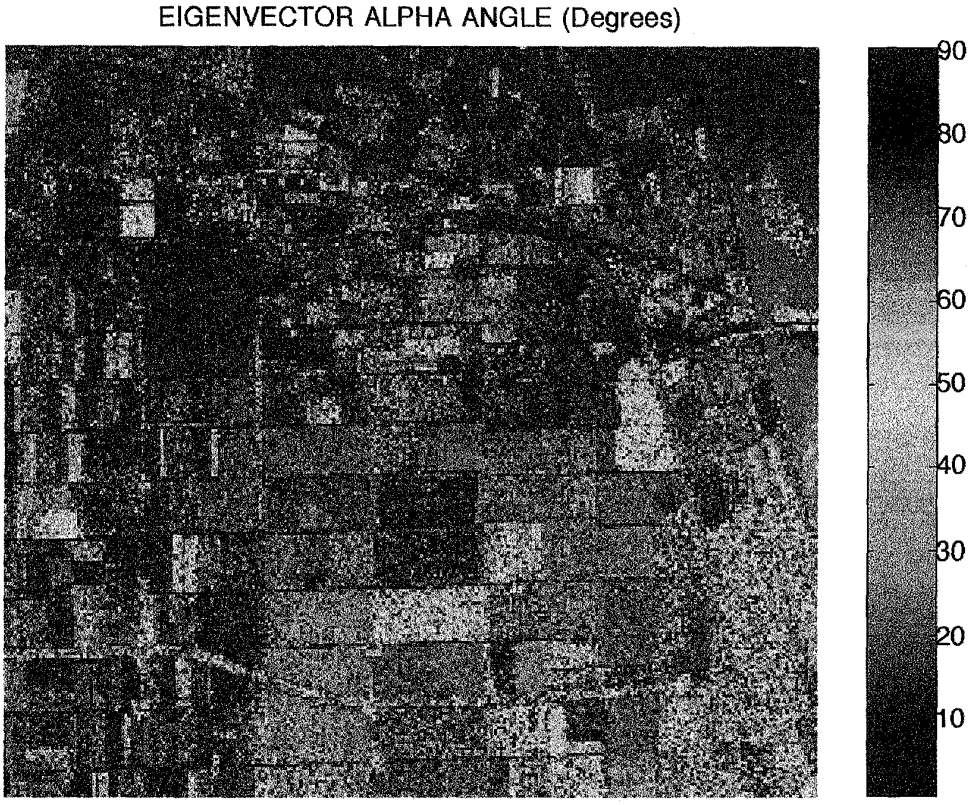

Fig. 14. Alpha angle image of L-band Flevoland AIRSAR data.

This follows from the observation that

$$[T]_{\text{obs}} = [\Psi]\underline{k}.\underline{k}^{*T}[\Psi]^{*T} \Rightarrow$$
$$[T]_{\text{obs}} = [T].*[\Sigma] \tag{83}$$

where the $.*$ operation represents element by element multiplication of the two matrices. In particular, if the speckle has a covariance matrix of the form shown in (84) (which implies that the speckle is random but completely polarized), then we can reduce the effect of the coherent noise by straightforward averaging of independent pixel coherency matrices:

$$[\Sigma] = \rho \begin{bmatrix} 1 & 1 & 1 & 1 \\ 1 & 1 & 1 & 1 \\ 1 & 1 & 1 & 1 \\ 1 & 1 & 1 & 1 \end{bmatrix}. \tag{84}$$

Such considerations drive us toward the use of the coherency matrix as discussed in earlier sections and away from the coherent approach adopted here. However, there would seem to be some place for these theorems in the case of high resolution low entropy scattering problems, where the coherent decomposition could be applied to the dominant eigenvector of the average coherency matrix $[T]$.

We can generalize the coherent TD concept by considering in advance the types of target components expected in the image, e.g., backscatter from sharp edges or corners with prescribed orientation, and then use a Gram–Schmidt (GS) orthogonalization to generate an orthonormal basis.

When we carry out this GS procedure our original targets will be distorted (unless we are fortunate to choose an orthonormal set to start with, such as the Pauli matrices themselves).

The above general coherent TD procedure is useful if only one dominant target component is expected (e.g., a dihedral or perhaps an edge contribution) and the other components are provided in support for constructing a suitable basis for the whole space of targets.

VIII. Application to Polarimetric SAR Data

To illustrate the potential of TD theorems for application to imaging radar data classification, we show an example processed image from the NASA/JPL AIRSAR data base. We choose an L-band image of a mixed agricultural scene in Flevoland, The Netherlands, collected in August 1989. This scene is chosen because of its flat topography, varied terrain cover and large field area. The eigenvector parameters are estimated locally using a 4×3 (azimuth $\times$ range) window. Since each original pixel is a 4-look measurement, then each pixel in the images shown is calculated from an effective 48-look average coherency matrix.

Fig. 13 shows an entropy image of the L-band SAR data. Notice that although many features have high entropy (and so

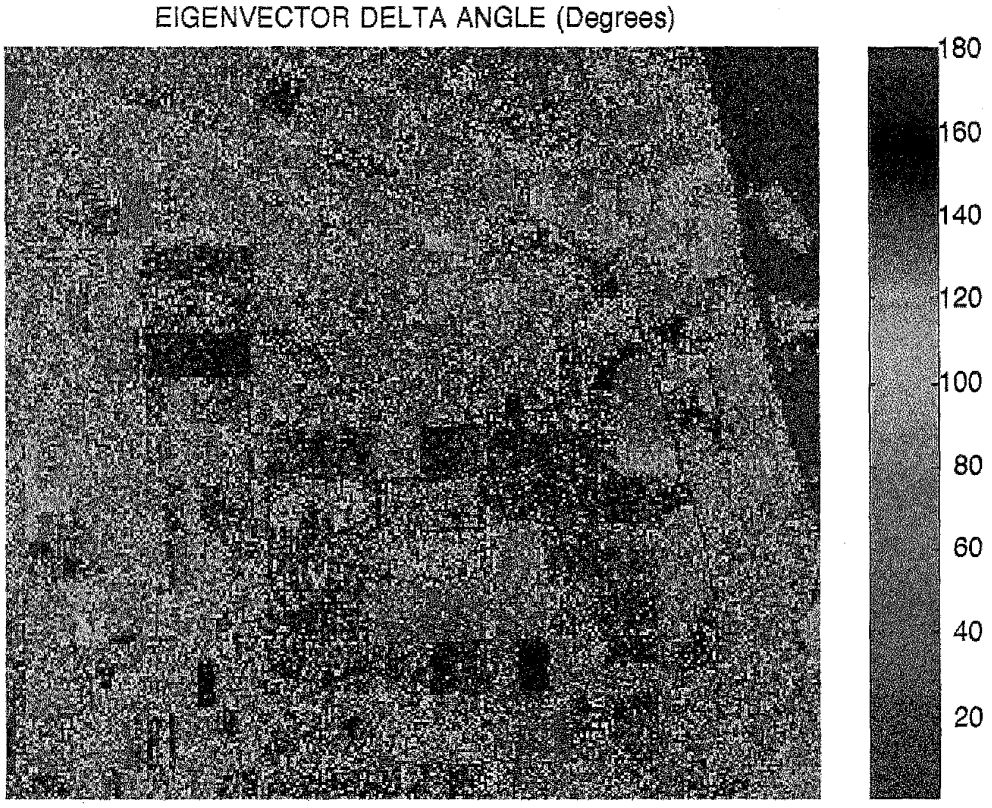

Fig. 15. Delta angle image of L-band Flevoland AIRSAR data.

reduced polarimetric information), there exist several distinct areas of both water and crop sites which have low entropy. This implies the possibility of reliable classification and parameter extraction from the polarimetric response of such targets [31].

Fig. 14 shows an image of the corresponding a parameter. Here we see a region which is largely blue, indicative of dominant single scattering ($\alpha = 0°$), except for localized but significant regions where the dominant scattering mechanism changes. This information is clearly different to that contained in the entropy image and reflects a physical basis for the presence of multiple scattering phenomena and spatial variation in the HH and VV scattered signal ratio.

Fig. 15 shows the third main classification parameter, the phase angle δ between $(HH + VV)$ and $(HH - VV)$. Here again we see that in different parts of the image the ratio $|HH/VV|$ changes, indicating different fundamental scattering mechanisms and providing a basis for classification (in red zones for example $|VV| > |HH|$ while in blue $|HH| > |VV|$). In yet other areas we see intermediate phase values indicating that the complex phase of HH and VV contains important information about the scattering mechanisms. Comparison with Fig. 13 indicates that these phase areas correspond to low entropy, and hence, must be considered as statistically significant.

These three examples show clearly how important physical information may be extracted from the coherency matrix, even in random media problems where there is considerable averaging. Other potential remote sensing examples have recently been presented in the literature [31], [48], [49], [52]. From these, it is clear that the entropy is a key parameter in establishing the accuracy with which parameters may be estimated from polarimetric observations and hence, in as much as any single parameter can do so, the entropy is an important indicator of the utility of polarimetry in remote sensing [31].

IX. Conclusion

In this paper, we have reviewed the theoretical basis for the application of target decomposition (TD) theorems to radar polarimetry. We have seen that there are three primary classes of such decompositions: Huynen type methods which attempt to extract a single scattering matrix from the averaged Mueller matrix (examples include the Chandrasekhar and Barnes/Holm decomposition). The Freeman decomposition may also be classed in this way, as it attempts to extract two single target components and a remainder from the observed covariance matrix.

A second class are represented by coherent theorems, where we attempt to decompose the *coherent* scattering matrix $[S_A]$ into the sum of elementary matrices (examples are the Krogager and Cameron decompositions). While these do not require estimates of the target coherency matrix, they are prone to problems from coherent speckle noise, from basis invariance and/or from lack of basis orthogonality.

The third and final class are represented by eigenvector decompositions of the coherency or covariance matrix. Examples are those presented by Cloude and van Zyl. We have shown the importance of constructing an orthonormal set of basis vectors for polarimetric problems and seen that for random targets the constraint of requiring statistical independence between components generates a natural basis from the eigenvectors of the coherency matrix, weighted by the eigenvalue spectrum. We have thus identified an important basis invariant parameterization in terms of three eigenvalues and a set of angles (obtained from the unitary eigenvectors). These parameters are related to physical scattering mechanisms in the scene and for the special case of reflection symmetry lead us to model the random media problem as a single scattering mechanism with a degree of disorder, the entropy, defined in the Von Neumann sense as a logarithmic sum of eigenvalues.

REFERENCES

[1] R. Touzi and A. Lopes, "The principle of speckle filtering in polarimetric SAR imagery," *IEEE Trans. Geosci. Remote Sensing,* vol. 32, pp. 1110–1114, Sept. 1994.

[2] J. R. Huynen, "Phenomenological theory of radar targets," Ph.D. dissertation, Technical Univ., Delft, The Netherlands, 1970.

[3] S. Chandrasekhar, *Radiative Transfer.* New York: Dover, 1960.

[4] L. Tsang, J. A. Kong, and R. T. Shin, *Theory of Microwave Remote Sensing.* New York: Wiley Interscience, 1985.

[5] V. Tatarinov, "Polarization radar: 15 years of development at the Siberian Scientific Polarization School," in *Proc. 3rd Int. Workshop on Radar Polarimetry (JIPR '95), IRESTE,* Univ. Nantes, France, Apr. 1995, pp. 348–353.

[6] W. M. Boerner, "Polarization dependence in electromagnetic inverse problems," *IEEE Trans. Antennas Propagat.,* vol. AP-29, pp. 262–274, Mar. 1981.

[7] A. B. Kostinski and W. M. Boerner, "On the foundations of radar polarimetry," *IEEE Trans. Antennas Propagat.,* vol. AP-34, pp. 1395–1404, Dec. 1986.

[8] S. R. Cloude, "Group theory and polarization algebra," *OPTIK,* vol. 75, no. 1, pp. 26–36, 1986.

[9] D. H. O. Bebbington, "Target vectors: Spinorial concepts," in *Proc. 2nd Int. Workshop on Radar Polarimetry,* IRESTE, Nantes, France, Sept. 1992, pp. 26–36.

[10] M. Born and E. Wolf, *Principles of Optics,* New York: Pergamon, 1989.

[11] C. V. M. van der Mee and J. W. Hovenier "Structure of matrices transforming Stokes parameters," *J. Math. Phys.,* vol. 33, no. 10, pp. 3574–3584, Oct. 1992.

[12] R. Barakat, "Bilinear constraints between the elements of the 4×4 Mueller–Jones Matrix of polarization theory," *Opt. Comms.,* vol. 38, pp. 159–161, Aug. 1981.

[13] D. G. M. Anderson and R. Barakat, "Necessary and sufficient conditions for a Mueller matrix to be derivable from a Jones matrix," *J. Opt. Soc. Amer. A,* vol. 11, pp. 2305–2319, Aug. 1994.

[14] M. I. Mishchenko, "Enhanced backscattering of polarized light from discrete random media: Calculations in exactly the backscattering direction," *J. Opt. Soc. Amer. A,* vol. 9, pp. 978–982, June 1992.

[15] M. P. van Albada, M. B. van der Mark, and A. Lagendijk, "Polarization effects in weak localization of light," *J. Phys. D,* vol. 21, no. 105, pp. 28–31, Oct. 1988.

[16] S. R. Cloude, "Uniqueness of target decomposition theorems in radar polarimetry," in *Direct and Inverse Methods in Radar Polarimetry, Part 1, NATO-ARW,* W. M. Boerner *et al.,* Eds. Norwell, MA: Kluwer, 1992, pp. 267–296.

[17] R. M. Barnes, "Roll-invariant decompositions of the polarization covariance matrix," Lincoln Lab., M.I.T., Lexington, Internal Rep., 1988.

[18] J. R. Huynen, "Comments on radar target decomposition theorems," P. Q. Res., Los Altos Hills, CA, Rep. PQR 105, Aug. 1988.

[19] E. Luneburg, "Canonical bases and the Huynen decomposition," in *Proc. 3rd Int. Workshop on Radar Polarimetry (JIPR '95),* IRESTE, Univ. Nantes, France, Apr. 1995, pp. 75–84.

[20] S. H. Nghiem, R. Yueh, Kwok, and F. K. Li, "Symmetry properties in polarimetric remote sensing," *Radio Sci.,* vol. 27, no. 5, pp. 693–711, Oct. 1992.

[21] H. Mott, *Antennas for Radar and Communications.* New York: Wiley, 1992.

[22] S. R. Cloude, "Radar target decomposition theorems" *Inst. Elect. Eng. Electron. Lett.,* vol. 21, no. 1, pp. 22–24, Jan. 1985.

[23] W. A. Holm and R. M. Barnes, "On radar polarization mixed state decomposition theorems," in *Proc. 1988 USA National Radar Conf.,* Apr. 1988, pp. 248–254.

[24] L. M. Novak, M. C. Burl, R. D. Chaney, and G. J. Owirka, "Optimal processing of polarimetric synthetic aperture radar imagery," *Lincoln Lab. J.,* vol. 3, no. 2, pp. 273–230, 1990.

[25] J. D. Klein and A. Freeman, "Quadpolarization SAR calibration using target reciprocity," *J. Electromagn. Waves Applicat.,* vol. 5, pp. 735–751, 1991.

[26] K. Tragl, "Polarimetric radar backscattering from reciprocal random targets," *IEEE Trans. Geosci. Remote Sensing,* vol. 28, pp. 856–864, 1990.

[27] S. R. Cloude, "Lie groups in electromagnetic wave propagation and scattering," *J. Electromagn. Waves Applicat.,* vol. 6, no. 8, pp. 947–974, 1992.

[28] A. Freeman, "SAR calibration: An overview," *IEEE Trans. Geosci. Remote Sensing,* vol. 30, no. 6, pp. 1107–1122, Nov. 1992.

[29] E. Luneburg, M. Chandra, and W. M. Boerner, "Random target approximations," in *Proc. PIERS '94,* Noordwijk, The Netherlands, July 1994, p. 247.

[30] D. S. Wiersma, M. P. van Albada, and A. Lagendijk, "Precise weak localization experiments reveal recurrent light scattering in random structures," in *Proc. PIERS '94,* Noordwijk, The Netherlands, July 1994, p. 192.

[31] S. R. Cloude, "An entropy based classification scheme for polarimetric SAR data," in *Proc. IGARSS '95,* Florence, Italy, July 1995, pp. 2000–2002.

[32] A. Freeman and S. Durden, "A three component scattering model to describe polarimetric SAR data," *Radar Polarimetry,* vol. SPIE-1748, pp. 213–225, 1992.

[33] A. Freeman, S. Durden, and R. Zimmerman, "Mapping sub-tropical vegetation using multi-frequency multi-polarization SAR data," in *Proc. IGARSS,* Houston, TX, June 1992, pp. 1686–1689.

[34] H. C. van de Hulst, *Light Scattering by Small Particles.* New York: Dover, 1981.

[35] J. J. van Zyl, "Application of Cloude's target decomposition theorem to polarimetric imaging radar data," *Radar Polarimetry,* vol. SPIE-1748, pp. 184–212, 1992.

[36] M. Ferri, L. Castellano, A. Siciliano, R. Vigliotti, and P. Murino, "Using polarimetric SAR data in morphological analyses: The Island of Ischia (Southern Italy)," in *Proc. IGARSS '94,* Pasadena, CA, July 1994 (paper 341130 on CD-ROM of the Proc.).

[37] M. C. Dobson, F. T. Ulaby, T. Le Toan, A. Beaudoin, E. S. Kasischke, and N. Christenson, "Dependence of radar backscatter on coniferous forest biomass," *IEEE Trans. Geosci. Remote Sensing,* vol. 30, pp. 412–415, Mar. 1992.

[38] T. Le Toan, A. Beaudoin, J. Riom, and D. Guyon, "Relating forest biomass to SAR data," *IEEE Trans. Geosci. Remote Sensing,* vol. 30, pp. 403–411, Mar. 1992.

[39] E. J. Rignot, S. J. Ostro, J. J. van Zyl, and K. C. Jezek, "Unusual radar echoes from the Greenland ice sheet," *Science,* vol. 261, pp. 1710–1713, 1993.

[40] E. Krogager, "A new decomposition of the radar target scattering matrix," *Electron. Lett.,* vol. 26, no. 18, pp. 1525–1526, 1990.

[41] E. Krogager and A. Freeman, "Three component break-downs of scattering matrices for radar target identification and classification," in *Proc. PIERS '94,* Noordwijk, The Netherlands, July 1994, p. 391.

[42] E. Krogager and Z. H. Czyz, "Properties of the sphere, diplane, helix decomposition," in *Proc. 3rd Int. Workshop on Radar Polarimetry (JIPR '95),* IRESTE, Univ. Nantes, France, Apr. 1995, pp. 106–114.

[43] E. Krogager, J. Dall, and S. N. Madsen, "Properties of the sphere, diplane, helix decomposition," in *Proc. 3rd Int. Workshop on Radar Polarimetry (JIPR '95),* IRESTE, Univ. Nantes, France, Apr. 1995, pp. 621–625.

[44] W. L Cameron and L. K. Leung, "Feature motivated polarization scattering matrix decomposition," in *Proc. IEEE Int. Radar Conf.,* Arlington, VA, May 7–10, 1990, pp. 549–557.

[45] ——, "Identification of elemental polarimetric scatterer responses in high resolution ISAR and SAR signature measurements," in *Proc. 2nd Int. Workshop on Radar Polarimetry (JIPR '92),* IRESTE, Nantes, France, Sept. 1992, pp. 196–212.

[46] L. M. Novak and M. C. Burl, "Optimal speckle reduction in polarimetric SAR imagery," *IEEE Trans. Aerosp. Electron. Syst.,* vol. 26, pp. 293–305, Mar. 1990.

[47] J. S. Lee, M. R. Grines, and S. A. Mango, "Speckle reduction in multipolarization, multifrequency SAR imagery," *IEEE Trans. Geosci. Remote Sensing,* vol. 29, pp. 535–544, July 1991.
[48] C. Unal and L. P. Ligthart, "Target decomposition theorems applied to rain," in *Proc. 3rd Int. Workshop on Radar Polarimetry (JIPR '95), IRESTE,* Univ. Nantes, France, Apr. 1995, pp. 99–105.
[49] M. I. Mishchenko and J. W. Hovenier, "Depolarization of light backscatterd by randomly oriented nonspherical particles," *Opt. Lett.,* vol. 20, no. 12, pp. 1356–1359, June 1995.
[50] S. R. Cloude, "Physical realisability of matrix operators in polarimetry," *SPIE, Polarisation Considerations Opt. Syst. II,* vol. 1166, pp. 177–185, Aug. 1989.
[51] S. R. Cloude and E. Pottier, "The concept of polarization entropy in optical scattering," *Opt. Eng.,* vol. 34, no. 6, pp. 1599–1610, 1995.
[52] D. Bicout and C. Brosseau, "Multiply scattered waves through a spatially random medium: Entropy production and depolarization," *J. Phys. I France,* vol. 2, pp. 2047–2063, Nov. 1992.

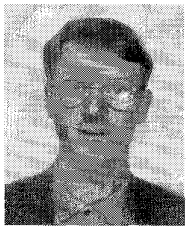

Shane Robert Cloude (M'88) received the B.Sc. degree from the University of Dundee, Scotland, in 1981 and the Ph.D. degree from the University of Birmingham, England, in 1987.

He is currently an Associate Professor at IRESTE, which is an Engineering School of the University of Nantes, France. Before his current position, he held teaching and research posts at the University of Dundee and the University of York, England. He has published more than 50 research papers, mainly on the subject of electromagnetic scattering and polarimetry. His main current research interests are in active remote sensing, radar imaging techniques, and time domain methods for computational electromagnetics.

Dr. Cloude is a Chartered Engineer, a member of the Electromagnetics Academy, the Optical Society of America (OSA), and the Institute of Electrical Engineers (IEE).

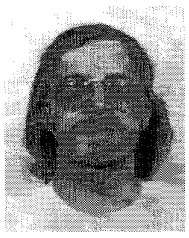

Eric Pottier (M'95) was born in Flers de l'Orne, France, in 1962. He received the "Signal Processing and Telecommunications" D.E.A. degree in 1987 and the Ph.D. degree in 1990, both from the University of Rennes, France.

In 1988, he joined the laboratory "Systemes et Signaux Hautes Frequencies" at IRESTE, University of Nantes, France, where he was Research and Teaching Assistant, involved in analog electronic and microwave systems. From 1991, he has held an Associate Professor position. His current activities of research and education are centered in the topics of analog electronic, microwave theory, and radar imaging with emphasis in radar polarimetry. Since November 1994, he has been the Head of "Radar Polarimetry Group" of the SEI (Systemes Electroniques et Informatiques) Laboratory, which is associated with CNRS (EP 0063). He has more than 40 publications in the area of radar polarimetry and has supervised 14 research students to graduation.